Ethanol stimulates locomotion via a G$_{αs}$-signalling pathway in IL2 neurons in *C. elegans*

James R. Johnson[*,†]**, Mark R. Edwards**[*]**, Huw Davies**[*]**, Daniel Newman**[*]**, Whitney Holden**[*]**, Rosalind E Jenkins**[‡]**, Robert D. Burgoyne**[*]**, Robert J. Lucas**[†] **and Jeff W. Barclay**[*]

[*]The Physiological Laboratory, Institute of Translational Medicine, University of Liverpool, Liverpool, L69 3BX, UK

[†]Faculty of Biological and Medical Sciences, University of Manchester, Manchester, M13 9PT, UK

[‡]Department of Molecular and Clinical Pharmacology, Institute of Translational Medicine, University of Liverpool, Liverpool, L69 3BX, UK

Running title: Ethanol stimulates locomotion

All correspondance to: J.W. Barclay; Tel: +44-151-794-5307; Fax: +44-151-794-5337; email: barclayj@liverpool.ac.uk

Abstract

Alcohol is a potent pharmacological agent when consumed acutely at sufficient quantities and repeated overuse can lead to addiction and deleterious effects on health. Alcohol is thought to modulate neuronal function through low affinity interactions with proteins, in particular with membrane channels and receptors. Paradoxically, alcohol acts as both a stimulant and a sedative. The exact molecular mechanisms for the acute effects of ethanol on neurons, as either a stimulant or a sedative, however remain unclear. We investigated the role that the heat shock transcription factor, HSF-1, played in determining a stimulatory phenotype of *Caenorhabditis elegans* in response to physiologically relevant concentrations of ethanol (17 mM; 0.1% v/v). Using genetic techniques we demonstrate that either RNAi of *hsf-1* or use of an *hsf-1(sy441)* mutant lacked the enhancement of locomotion in response to acute ethanol exposure evident in wild-type animals. We identify that the requirement for HSF-1 in this phenotype was IL2-neuron specific and required the downstream expression of the α-crystallin orthologue HSP-16.48. Using a combination of pharmacology, optogenetics and phenotypic analyses we determine that ethanol activates a $G_{\alpha s}$ – cAMP – protein kinase A signalling pathway in IL2 neurons to stimulate nematode locomotion. We further implicate the phosphorylation of a specific serine residue (Ser322) on the synaptic protein UNC-18 as an end-point for the $G_{\alpha s}$-dependent signalling pathway. These findings establish and characterise a distinct neurosensory cell signalling pathway that determines the stimulatory action of ethanol and identifies HSP-16.48 and HSF-1 as novel regulators of this pathway.

Introduction

Alcohol is one of the most prevalent addictive substances and its overuse produces a severe burden on society (Who 2011). Acute effects of alcohol include motor incoordination, sedation and anaesthesia. Alcohol also acts as a stimulant, activating neurotransmitter release within the brain's reward circuitry, increasing heart rate and inducing aggression and risk-taking (Hendler *et al.* 2013). The cellular mechanisms underlying either the anaesthetic or stimulatory effects of ethanol are only now being elucidated. Ethanol was initially hypothesised to act through indirect perturbations of the lipid environment thereby affecting broadly all membrane protein function (Harris *et al.* 2008). Recent work instead implicates more direct effects on specific protein targets, particularly membrane proteins such as ion channels and receptors (Howard *et al.* 2014; Trudell *et al.* 2014). Ethanol has a very simple molecular structure and is thought to exert its intoxicating effects through interactions with these target proteins with very low affinity (~0.1M) to alter the natural dynamics of protein function (Howard *et al.* 2011; Olsen *et al.* 2014). A complete understanding of both the acute and chronic effects of alcohol within the nervous system is an important unresolved question in physiology.

Invertebrates are excellent genetic models for identification of cellular/molecular mechanisms governing the sedative properties of ethanol and other anaesthetics (Barclay *et al.* 2010; Devineni and Heberlein 2013; Bettinger and Davies 2014). In *Drosophila*, studies of acute ethanol intoxication have implicated a large number of proteins and signalling pathways (Kaun *et al.* 2012). In *Caenorhabditis elegans*, proteins such as Munc18 and Rab3 (Kapfhamer *et al.* 2008; Graham *et al.* 2009; Johnson *et al.* 2013), the BK channel *slo-1* (Davies *et al.* 2003), the leak channel regulator *Lightweight* (Speca *et al.* 2010), chloride intracellular channels (Bhandari *et al.* 2012) and the α-crystallin orthologue HSP-16.48 (Johnson *et al.* 2016) all affect sensitivity to high levels of ethanol (400mM). The use of

very high external ethanol in *C. elegans* behavioural analysis is thought to be a consequence of poor penetration through the nematode cuticle (Alaimo *et al.* 2012). Indeed, internal concentrations in response to 400mM external ethanol are estimated between 20 and 60mM (Alaimo *et al.* 2012; Johnson *et al.* 2016), although not all studies are in agreement (Mitchell *et al.* 2007). In addition to sedation, at lower concentrations ethanol acts as a stimulant (Phillips and Shen 1996; Wolf *et al.* 2002; Balino *et al.* 2016). In *C. elegans*, ethanol-induced stimulation occurs at external concentrations (17 mM, 0.1%) whose absolute values would be physiologically consistent with blood alcohol limits for impaired driving (House of Commons Transport Committee 2010). Acute exposure of nematodes to 17 mM ethanol causes a small, but characteristic increase in locomotion rate (Graham *et al.* 2009; Johnson *et al.* 2013). Virtually nothing is known about the cellular and molecular basis underlying *C. elegans* phenotypes at this ethanol concentration.

Heat shock activates a transcriptional response to toxic insults whereby protective cellular chaperone (heat shock protein; HSP) expression is increased under the control of the heat shock transcription factor (HSF1) (Anckar and Sistonen 2011). The HSF1-HSP pathway is also ubiquitously involved in stress-independent cellular functions such as polypeptide folding, protein-protein interactions (Kampinga and Craig 2010) and proteostasis (Morimoto 2011) as well as contributing to diseases like cancer (Mendillo *et al.* 2012) and neurodegeneration (Kondo *et al.* 2013). In *C. elegans* RNAi or *loss-of-function* mutations of *hsf-1* increase stress sensitivity, but also accelerate ageing (Hsu *et al.* 2003; Prahlad *et al.* 2008; Baird *et al.* 2014). We have recently shown that *hsf-1 loss-of-function* increases sensitivity to 400 mM ethanol (Johnson *et al.* 2016). This hypersensitivity was partially the result of the downstream basal expression of HSP-16.48, an orthologue of the human small heat shock protein α-crystallin, in a process unrelated to an HSF-1-dependent heat shock stress response. Here, we identify that the stimulatory ethanol phenotype also required HSF-

1, but specifically in 6 IL2 chemosensory neurons and could be completely rescued by transgenic expression of HSP-16.48 in IL2 neurons of the *hsf-1* mutant. Using a combination of pharmacology, genetics and optogenetics, we determined further that this ethanol-dependent stimulation of motility acts via a $G_{\alpha s}$-cAMP-protein kinase A signalling pathway within the IL2 sensory neurons and identifies the exocytotic protein UNC-18 as a downstream effector for PKA. Although individual components of the $G_{\alpha s}$ pathway have been linked previously to the neuronal effects of ethanol, this study uniquely characterises the entire signalling pathway in ethanol-dependent stimulation.

Materials and Methods

Nematode culturing, strains and genetics. *C. elegans* were cultured under standard conditions at 20°C on Nematode Growth Media (NGM) agar plates with OP50 *E. coli* as a food source as previously described (Brenner 1974; Graham *et al.* 2009; Edwards *et al.* 2012). These experiments used the following strains: Bristol N2 (wild-type), PS3551 *hsf-1(sy441)*, KG524 *gsa-1(ce94)*, KG421 *gsa-1(ce81)*, MT363 *goa-1(n363)*, NM1380 *egl-30(js126)*, KG1180 *lite-1(ce314)* and NL2099 *rrf-3(pk1426)*. To investigate effects of single-copy transgenic rescue of *hsf-1(sy441)* mutants we analysed the OG532 (*hsf-1(sy441);drSi13[hsf-1p::hsf-1::GFP::unc-54 3'UTR + Cbr-unc-119(+)]*) and OG580 (*hsf-1(sy441);drSi28[hsf-1p::hsf-1(R145A)::GFP::unc-54 3'UTR + Cbr-unc-119(+)]*) strains (Morton and Lamitina 2013) which are single-copy MosSCI-produced rescues of the *hsf-1(sy441)* mutant. Basal locomotion rates for each strain can be found in Table S1. Transgenic animals were derived by germline injection as previously described (Mello *et al.* 1991; Graham *et al.* 2009; Edwards *et al.* 2012). All injections were performed with 10 ng/µl indicated construct) and 30 ng/µl (indicated co-injection marker) and made up to 100 ng/µl total with empty filler DNA (either pUC19 or pBluescript). For each transgenic strain, 3 independent lines were isolated and tested phenotypically. The results presented were consistent for all individual lines; however, individual line results can be found in Table S2. Transgenic lines used in this study include the following: N2;*ulvEx[P$_{hsf-1}$::hsf-1]*, N2;*ulvEx[P$_{rab-3}$::hsb-1]*, N2;*ulvEx[P$_{klp-6}$::hsb-1]*, N2;*ulvEx[P$_{rab-3}$::hsp-16.48]*; N2;*ulvEx[P$_{rab-3}$::hsp-16.48 Δ38-44]*, N2;*ulvEx[P$_{klp-6}$::hsp-16.48]*, N2;*ulvEx[P$_{unc-18}$::unc-18 S322A]*, N2;*ulvEx[P$_{klp-6}$::unc-18 S322A]*, N2;*ulvEx[P$_{klp-6}$::kin-1::P$_{klp-6}$]*, *hsf-1(sy441);ulvEx[P$_{hsf-1}$::hsf-1]*, *hsf-1(sy441);ulvEx[P$_{rab-3}$::hsf-1]*, *hsf-1(sy441);ulvEx[P$_{myo-3}$::hsf-1]*, *hsf-1(sy441);ulvEx[P$_{glr-1}$::hsf-1]*, *hsf-1(sy441);ulvEx[P$_{unc-17}$::hsf-1]*, *hsf-1(sy441);ulvEx[P$_{osm-6}$::hsf-1]*, *hsf-1(sy441);ulvEx[P$_{gcy-8}$::hsf-1]*, *hsf-1(sy441);ulvEx[P$_{klp-}$*

6::hsf-1], *hsf-1(sy441);ulvEx[P_{rab-3}::hsp-16.48]*, *hsf-1(sy441);ulvEx[P_{rab-3}::hsp-16.48 Δ38-44]* and *hsf-1(sy441);ulvEx[P_{klp-6}::hsp-16.48]*. Transgenic constructs in Bristol N2 were co-expressed with either a *P_{sur-5}::GFP* or a *P_{rab-3}::GFP* marker. To indicate appropriate cellular expression for additional cell-tissue specific promoters, each of these transgenics used a GFP co-expression marker under the control of the same promoter. IL2 neurons were visualised with the promoter::GFP reporter *hsf-1(sy441);ulvEx[P_{klp-6}::GFP; P_{myo-2}::mCherry]*. To examine cell-specific RNAi, Bristol N2 worms were injected with the plasmid *P_{klp-6}::kin-1::P_{klp-6}*, which drove cell-specific expression of *kin-1* (catalytic subunit of *C. elegans* protein kinase A) in both the forward and reverse direction (Esposito *et al.* 2007).

RNAi experiments. RNAi experiments were performed using the *rrf-3(pk1426)* strain. RNAi was induced by feeding (Kamath and Ahringer 2003) using the ORFeome-based RNAi library (Rual *et al.* 2004) as described previously (Johnson *et al.* 2016). HT115 RNAi bacteria were cultured in LB media with 100 μg/ml ampicillin and spotted onto 60 mm diameter NGM plates supplemented with 1 mM isopropyl β-1-thiogalactopyranoside (IPTG) and 25 μg/ml carbenicillin. NGM plates were dried for 4 days before spotting. 5 L3-L4 worms were added to each RNAi plate and cultured at 20°C. Phenotypic analysis was performed on first generation progeny fed with the indicated RNAi bacterial clones. For the negative control for the RNAi screen, worms were fed with an empty feeding vector.

Cloning. *C. elegans* genes of interest were amplified from either Bristol N2 genomic DNA (*hsp-16.48*) or cDNA (*hsf-1*), cloned into pDONR201 and recombined into DEST vectors to create tissue-specific expression vectors, as previously described (Johnson *et al.* 2016). For *hsb-1*, the gene was amplified from Bristol N2 genomic DNA using the following primers:

hsb-1 attB forward:

GGGGACAAGTTTGTACAAAAAAGCAGGCTTCATGTCCGATGAGAAGTCTACC

hsb-1 AttB reverse:

GGGGACCACTTTGTACAAGAAAGCTGGGTCTTATTGAGCGCTTGGCGGATGTTC

Mutagenesis of the *hsp-16.48* gene was performed using the Q5 Site-Directed Mutagenesis Kit (New England BioLabs) as per the manufacturer's instructions. The *unc-18* S322A expression vector was created using the Gene Tailor mutagenesis kit (Invitrogen) from a vector carrying the *unc-18* cDNA under the control of the *unc-18* genomic flanking regions (gift from Dr. H. Kitayama, Kyoto University, Japan) (Gengyo-Ando *et al.* 1996). To create the $P_{klp-6}::unc-18$ construct, the existing *unc-18* promoter was excised by EcoRI and BamHI restriction digest and replaced with *klp-6* promoter using the NEBuilder DNA assembly (New England BioLabs). For glutathione-S-transferase (GST) fusion protein production, *unc-18* was subcloned into pGEX-6p-1 as previously described (Edwards *et al.* 2012).

All *C. elegans* promoter fragments were amplified from Bristol N2 genomic DNA and cloned into pPD117.01 (kind gift of A. Fire, Stanford University) in place of P_{mec-7}. These vectors were converted into Gateway DEST vectors using a conversion cassette (Life Technologies). P_{rab-3} (kind gift of M. Nonet, Washington University in St. Louis), P_{myo-3} (kind gift of A. Fire, Stanford University) and P_{hsf-1} are previously described (Edwards *et al.* 2012; Johnson *et al.* 2016). The following primers were used for additional promoter cloning:

P_{unc-17} forward: AGTCGGCGCGCCATCCGTTCCCATCCGCTTCATC

P_{unc-17} reverse: AGGAGGATCCGGTTACTATTTTGAACAAGAGATGCGG

P_{glr-1} forward: AGTCGGCGCGCCCTGTAGCCGGTATGCACTGATAAC

P_{glr-1} reverse: AGTCGGATCCTGTGAATGTGTCAGATTGGGTG

P_{osm-6} forward: ATGTGGCGCGCCCAGTGGAATCACCATTGGGTATCCAG

P~osm-6~ reverse: GGGTGGATCCGAAGGTAATAGCTTGAAAGAGATATAAGCCC

P~gcy-8~ forward: AGTCGGCGCGCCAACTACCTTCCTCCGCGTCC

P~gcy-8~ reverse: AGTCGGATCCTTTGATGTGGAAAAGGTAGAATCG

P~klp-6~ forward: CCCCGGCGCGCCAACGTCCCAGACAATTTCAAC

P~klp-6~ reverse: CTACGGATCCGGAGTCACCCTTTCCCCTTATTCTG

The *P~klp-6~::kin-1::P~klp-6~* construct was made as follows. A 750 bp fragment of *kin-1* was amplified from the Vidal library clone (Rual *et al.* 2004) and sub-cloned into the *P~klp-6~::*GFP expression vector, downstream of *P~klp-6~* in place of GFP, using the NEBuilder cloning kit (New England BioLabs). The *P~klp-6~::kin-1* PCR fragment was then amplified from this construct and again sub-cloned into the same *Pklp-6* construct as before, but in reverse. Correct construction was confirmed by PCR and sequencing. Primers used were as follows:

kin-1 RNAi fwd: CTATCGATTCGCGGCCATCACAAGTTCGAATCGGA

kin-1 RNAi rev (step 1): CTTGTGGGCTTTTGTATAGTTCGTCCGGATAAC

kin-1 RNAi rev (step 2): CTATCGATTCGCGGCCATCACAAGTTGGATAACTAC

Protein phosphorylation and mass spectrometry: For *in vitro* biochemistry, recombinant proteins (GST, GST-UNC-18) were produced as described previously (Edwards *et al.* 2012). For phosphorylation experiments, 2 μg of substrate protein was incubated with 2 U of PKA catalytic subunit (Sigma), 100 μM ATP and 2 μCi [γ-^{32}P]ATP (GE Healthcare) in a 50 μl final reaction volume of MES buffer (50 mM MES, 10 mM MgCl$_2$, 1 mM DTT, 0.5 mM EDTA, pH 6.9). Reactions were incubated at 30°C for 3 hours before termination. To determine phosphorylation, 20 μl of the kinase reaction was separated by SDS-PAGE, stained with Coomassie Blue dye, destained overnight in destainer (35% ethanol, 2% glycerol (v/v)),

air-dried in Hoeffer Easy Breeze plastic frames (Thermo Fisher Scientific), exposed to a

phosphor screen for 2-4 hours and scanned by a PhosphorImager 425 (Molecular Dynamics).

For *in vitro* phosphorylation site determination, phosphorylated samples were separated on

NuPAGE 4-12% Bis-Tris precast gels (Invitrogen) and stained with Coomassie Blue dye

before excision of protein bands. Gel plugs were destained in 50% acetonitrile (v/v)/50 mM

ammonium bicarbonate and dried before incubation in trypsin (5 ng/μl in 50 mM ammonium

bicarbonate) for 16 hours at 37°C. Peptides were then extracted by sonication of gel plugs in

60% (v/v) acetonitrile/1% (v/v) trifluoroacetic acid. Extracts were thoroughly dried and

ZipTipped (Millipore) before electrospray ionisation mass spectrometry (MS). Residual

peptides were resuspended in 50% (v/v) acetonitrile/0.05% trifluoroacetic acid, and 5 μl of

suspension was delivered into a QStar Pulsar I hybrid quadrupole time-of-flight MS (AB

Sciex) by automated in-line liquid chromatography (integrated LCPackings System, 5 mm

C18 nano-precolumn and 75 μm X 15 cm C18 PepMap column (Dionex)). A gradient from 5

– 48% acetonitrile/0.05% trifluoroacetic acid (v/v) in 60 minutes was applied at a 300 nl/min

flow rate and survey scans of 1 s were acquired for m/z 400-2000. The most intense ions

were selected for tandem mass spectrometry (MS/MS) with 2 s accumulation times and a

dynamic exclusion of 30 s. Identification and analysis was performed using MASCOT

software (Matrix Science).

Optogenetics. JellyOp (Bailes *et al.* 2012) and hRh1 (Bailes and Lucas 2013) coding

domain sequences were PCR amplified from pcDNA3.1 and pcDNA3.5 expression vectors

respectively and sub-cloned downstream of P_{klp-6} in pPD117.01 (detailed above) via Gibson

Cloning techniques (NEB, UK). The optogenetic vectors were then transformed by germline

injection into *C. elegans* as described above. The vectors were expressed in the *lite-1(ce314)*

background to prevent any potential photophobic responses (Husson *et al.* 2013). All

optogenetic worms strains were then grown in the dark at 20°C on standard NGM plates with

OP50 bacteria as a food source. One day prior to assays, late L4 worms were picked onto standard 60 mm NGM plates with 50 μl OP50 supplemented with 100 μM 9-cis-Retinal, an active chromophore for opsin. All plates and worms were handled either in the dark or under a dim red light (>630 nm). Thrashing assays were performed under the dim red light in Dent's solution (140 mM NaCl, 6 mM KCl, 1 mM $CaCl_2$, 1 mM $MgCl_2$, 5 mM Hepes, pH 7.4, with bovine serum albumin at 0.1 mg/ml), in the presence or absence of 17 mM ethanol, using a Leica MZ10F-stereomicroscope (Leica, UK) equipped with a pE-300 LED fluorescence light source (CoolLED, UK). To activate opsin, worms were illuminated with a single flash of 100% power green LED through the ET GFP filter set for 5 seconds. For hRh1, opsin activation occurred as soon as they were placed in the Dent's solution and thrashing was quantified after 10 minutes acclimation (as below). For JellyOp, worms were illuminated following the 10 minutes acclimation in Dent's solution just prior to thrashing quantification, as the JellyOp activation is more transient (Bailes *et al.* 2012). Assays were repeated on three separate days to confirm replicability.

Behavioural Assays. Phenotypic analysis was performed in a temperature controlled room on young adult hermaphrodites from sparsely populated plates grown at 20°C. Unless otherwise indicated, experiments were conducted at an ambient temperature of 20°C. Here, locomotion rate was measured as thrashing (Gjorgjieva *et al.* 2014) in 200 μl Dent's solution as previously described (Graham *et al.* 2009; Johnson *et al.* 2013). One thrash was defined as a complete movement from maximum to minimum amplitude and back again. For acute ethanol experiments, ethanol was diluted to 17 mM in Dent's solution and locomotion was quantified following 10 minutes exposure and normalised as a percentage of the mean thrashing rate of untreated worms measured each day (at least 10 control worms per strain). For forskolin (Sigma) experiments, forskolin was diluted in dimethyl sulfoxide (DMSO) and added to Dent's solution in the indicated concentration. For direct comparison in these

experiments, control (untreated) worms were exposed to Dent's with an equal concentration of DMSO. H-89 (Sigma) was diluted in water and added to the Dent's/DMSO solution in the indicated concentration. For chemotaxis assays (Kashyap *et al.* 2014), experimental assay plates (100 mm Petri dishes) contained 2% (w/v) agar, 5 mM KH_2PO_4, 1 mM $CaCl_2$, 1 mM $MgSO_4$. Plates were poured 3 days prior to use and allowed to dry. Worms were washed in M9 buffer and placed on the centre of the plate. One microliter of the attractant (100% ethanol) and a negative control (distilled water) were pipetted on opposite sides of the plate. The number of worms on either side of the plate was calculated following 90 minutes. The chemotaxis index (C.I.) was calculated as C.I. = (# worms at attractant - # worms at control) / total number of worms. For worm avoidance assays, a 0.9 cm ring of a substance was made by a stamping procedure on unseeded NGM plates. Immediately after stamping, 30 worms were placed within the centre of the ring, completed within 2 minutes. Following 10 minutes exposure, the number of worms that had crossed the ring was counted.   In preliminary experiments, 0.9 cm was found sufficient to permit most worms to cross a neutral substance (distilled water) within 10 minutes. All data are expressed as mean ± SE. As indicated, significance was tested by Student's t-test, Mann-Whitney U-test or analysis of variance (ANOVA) with Tukey post-hoc comparisons where appropriate.

Data Availability. Strains are available upon request.

Results

HSF-1, the heat shock transcription factor, is involved in a plethora of cellular

functions (Anckar and Sistonen 2011; Morimoto 2011; Vihervaara and Sistonen 2014). In *C.*

elegans, the *hsf-1(sy441)* allele is a viable *loss-of-function* point mutation in the *hsf-1* gene

that acts as an inhibitor of HSF-1 transcriptional activity (Hajdu-Cronin *et al.* 2004),

increasing temperature sensitivity and decreasing lifespan (Baird *et al.* 2014). Nematodes

respond to high external ethanol concentration (400 mM) by a dose-dependent decrease in

coordinated locomotion (Davies *et al.* 2003; Graham *et al.* 2009) and we have recently

characterised a novel role for HSF-1 in determining this phenotype (Johnson *et al.* 2016).

Additionally, however, worms respond phenotypically to low levels of external ethanol (17

mM) with a reproducible enhancement in locomotor activity (Graham *et al.* 2009; Johnson *et*

al. 2013). In Bristol N2 wild-type worms, this stimulation is a 5-10% increase in basal

locomotion rate, as quantified by thrashing (Figure 1A). We tested whether the *hsf-1(sy441)*

mutation would also hypersensitise worms to the effects of low concentrations of ethanol.

Surprisingly, we found that the stimulatory effect of 17 mM external ethanol was completely

absent in worms containing the *hsf-1(sy441)* mutation (Figure 1A). The *hsf-1(sy441)* mutant

is well established to have a temperature-sensitive phenotype and we verified that the low

dose ethanol phenotype was not affected by the ambient temperature (Figure 1B); however,

all other described experiments were conducted at 20°C standard temperature.

HSF-1 is an ubiquitously expressed transcription factor that is active in all cell types;

however, the role of *hsf-1(sy441)* in the hypersensitivity to 400 mM external ethanol is

dependent upon pan-neuronal *hsf-1* expression (Johnson *et al.* 2016). We therefore

investigated next whether the ablation of the low (17 mM) ethanol stimulation of locomotion

phenotype observed in the *hsf-1(sy441)* mutant was also pan-neuronal in nature by tissue-

specific transgenic rescue. To allow for a direct comparison of the stimulatory effects of

ethanol independent of basal locomotor rates, the data are presented as thrashing rate

normalised to untreated worms of the same strain as done in previous studies (Davies *et al.*

2003; Graham *et al.* 2009; Johnson *et al.* 2016). Basal rates for all strains, however, can be

compared in Table S1. Whilst overexpression of *hsf-1* in Bristol N2 controls had no

additional effect, transgenic rescue of *hsf-1(sy441)* under its own promoter ($P_{hsf-1}::hsf-1$) or

specifically under the control of a pan-neuronal promoter ($P_{rab-3}::hsf-1$) completely rescued

the stimulatory ethanol phenotype (Figure 2A). Transgenic rescue of *hsf-1(sy441)* using a

body wall muscle promoter ($P_{myo-3}::hsf-1$), however, was insufficient to rescue. As a

complementary approach to investigate *hsf-1* function in the ethanol phenotype, we cloned

and overexpressed *hsb-1* in Bristol N2. *hsb-1* is a negative regulator for *hsf-1* transcriptional

function and it's overexpression in *C. elegans* results in similar phenotypes to *loss-of-*

function of *hsf-1* (Satyal et al. 1998). Overexpression of *hsb-1* pan-neuronally in Bristol N2

worms ($P_{rab-3}::hsb-1$) also resulted in a loss of ethanol stimulation of locomotion similar to

that seen in the *hsf-1(sy441)* mutant (Figure 2A). From these transgenic rescue experiments,

we conclude that the loss of the ethanol stimulation phenotype is a consequence of a loss in

neuronal *hsf-1* function.

As the *rab-3* promoter drives expression throughout the nervous system, we next

determined whether the stimulatory ethanol phenotype could be localised more precisely in

the nervous system. Intriguingly, the 17 mM ethanol stimulatory phenotype of *hsf-1(sy441)*

worms could be re-established by transgenic expression of wild-type *hsf-1* specifically in

cholinergic neurons ($P_{unc-17}::hsf-1$) or in ciliated sensory neurons ($P_{osm-6}::hsf-1$) but not in

interneurons ($P_{glr-1}::hsf-1$) or the AFD thermosensory neurons ($P_{gcy-8}::hsf-1$) (Figure 2A).

The localisation of the ethanol-induced stimulation of locomotion to either cholinergic

neurons or ciliated sensory neurons was particularly serendipitous, as these two promoters are

predicted to overlap in only 1 nematode cell type, the inner labial sensilla neurons, IL2

(Figure 2B). There are 3 pairs of IL2 neurons located in the head of the animal, all with ciliated endings (White *et al.* 1986; Burket *et al.* 2006). IL2 neurons are cholinergic (Zhang *et al.* 2014) and are predicted to be chemosensory as their dendrites are exposed to the external environment. Very little has been published ascribing function to the IL2 neurons; however, they do regulate nictation, a behaviour whereupon a nematode waves its head in three dimensions (Lee *et al.* 2012). We tested whether the absence of the stimulatory ethanol phenotype of *hsf-1(sy441)* could be reversed by transgenic expression of wild-type *hsf-1* specifically in the IL2 neurons. For this, we cloned the promoter region of the *klp-6* gene, which in hermaphrodites is expressed in the IL2 neurons specifically (Peden and Barr 2005). Localisation was verified by examination of a promoter::GFP transgenic worm, confirming that the IL2 neuronal structures appeared anatomically intact even in the *hsf-1*(*sy441*) mutant (Figure 2C), although an in depth ultrastructural analysis of the cilia in this mutant remains to be fully investigated. We then determined that expression of wild-type *hsf-1* in the IL2 neurons (P_{klp-6}::*hsf-1*) alone could restore the stimulatory ethanol phenotype of the *hsf-1(sy441)* mutant to a level indistinguishable from wild-type worms (Figure 2D). The complementary approach also confirmed that IL2-specific overexpression of *hsb-1* (P_{klp-6}::*hsb-1*), the negative regulator for *hsf-1*, was able to block the ethanol-induced stimulation in Bristol N2 (Figure 2D).

hsf-1(sy441) worms have a slightly lower basal locomotor rate (Fig. 1A); however, previous transgenic rescue experiments indicate that the basal locomotion rate is uncorrelated with the high ethanol phenotype (Johnson *et al.* 2016). Our data here also support a lack of correlation between basal locomotor rate and the low ethanol phenotype (Table S1). For example, IL2-neuron overexpression of *hsb-1* in Bristol N2 does not reduce basal locomotion rate at all, but does block the low ethanol phenotype. Alternatively, overexpression of wild-type *hsf-1* in IL2-neurons in the *hsf-1(sy441)* mutant background does not rescue the

locomotor defect of the mutant, but did restore the low ethanol phenotype. Notwithstanding this lack of correlation, we were interested in determining whether the reduced locomotor rate in the *hsf-1(sy441)* mutant was a consequence of the point mutation. The *hsf-1(sy441)* strain was originally isolated in a genetic screen of suppressors of heat shock induced expression, where it was both backcrossed and outcrossed (Hajdu-Cronin *et al.* 2004). We have demonstrated here (Table S1) and elsewhere (Johnson *et al.* 2016) that transgenic rescue can alter many *hsf-1*-dependent phenotypes, without altering the basal locomotor rates consistently indicating that the defect in locomotion may be independent of the *sy441* mutation or possibly incomplete rescue by the transgene. To address this question more directly, we analysed the OG532 strain which is a single copy MosSCI-integrated rescue of *hsf-1(sy441)* (Morton and Lamitina 2013). The OG532 strain demonstrated a significant, yet incomplete, rescue of the locomotion defect in comparison to Bristol N2 (Table S1). The incomplete rescue of the locomotion defect was reminiscent of a reported incomplete rescue of the *hsf-1(sy441)* temperature-sensitivity (Morton and Lamitina 2013). Reassuringly, the single-copy rescue did restore the ethanol stimulatory phenotype (Figure S1) to a level similar to that seen with transgenic overexpression. In contrast the OG580 strain, a single-copy rescue of *hsf-1(sy441)* with a DNA-binding defective mutant *hsf-1* (Morton and Lamitina 2013), impaired locomotion further (Table S1) and did not rescue the ethanol phenotype (Figure S1). These data indicate a potentially complex role for *hsf-1* in basal locomotor rate which is perhaps unsurprising given the broad cellular functions for the HSF-1 transcription factor and its downstream transcriptional targets. Critically, however, our results show that the basal locomotor rate is unrelated to the ethanol stimulatory effect and is instead a consequence of the *hsf-1(sy441)* mutation.

Our previous work on HSF-1 and its effect on sensitivity to 400 mM external ethanol indicated that the main effector for HSF-1 was the small heat shock protein HSP-

16.48 (Johnson *et al.* 2016). This work showed that RNAi of *hsp-16.48* phenocopied RNAi of *hsf-1* and that transgenic expression of *hsp-16.48* partially rescued the high dose ethanol sensitivity of the *hsf-1(sy441)* mutants. Finally, overexpression of *hsp-16.48* greatly reduced wild-type worm sensitivity to high external ethanol in a manner dependent upon an intact seven amino acid region of the N-terminus (amino acids 38-44) (Johnson *et al.* 2016). We next performed a series of experiments to test for functional similarities with the stimulatory ethanol phenotype. There unfortunately are no available *hsp-16.48* null mutations as the gene has undergone evolutionary genetic duplication rendering null mutations prohibitively difficult to isolate (Johnson *et al.* 2016). Our results showed that RNAi knockdown of *hsf-1* also resulted in a loss of the 17 mM ethanol phenotype (Figure 3A), to an extent similar to that seen with the *sy441* point mutation. Reminiscent of the sedative ethanol phenotype results (Johnson *et al.* 2016), RNAi of *hsp-16.48* also blocked the stimulatory ethanol phenotype to an equivalent level to *hsf-1* RNAi (Figure 3A). Distinct from the sedative ethanol phenotype (Johnson *et al.* 2016), however, transgenic expression of *hsp-16.48* either pan-neuronally (P_{rab-3}::*hsp-16.48*) or in IL2 neurons specifically (P_{klp-6}::*hsp-16.48*) was sufficient to restore completely the stimulatory ethanol phenotype in the *hsf-1(sy441)* mutant (Figure 3B). Finally, we determined that overexpression of *hsp-16.48* in Bristol N2 wild-types (P_{rab-3}::*hsp-16.48*) increased the effect of 17 mM external ethanol whereas the N-terminal truncation mutant (P_{rab-3}::*hsp-16.48 Δ38-44*) appeared to act as neomorphic or as dominant-negative (Figure 3C). Expression of the truncation mutant in the *hsf-1(sy441)* background, however, did not result in an enhancement of the ethanol-dependent reduction in locomotion in comparison to *hsf-1(sy441)* alone (Figure 3B). Therefore we hypothesise that the truncation mutant is possibly acting here as a dominant-negative. These experiments implicate HSP-16.48 in the stimulatory ethanol phenotype, acting downstream of HSF-1 in a manner requiring the seven amino acid region of the N-terminus.

As HSF-1/HSP-16.48 was acting in a chemosensory neuron to increase locomotion, we were interested to determine whether this increase in motility was reflective of either positive or negative chemotaxis. Indeed the performed thrashing assays immersed the animals directly into ethanol where it would be impossible to determine any directionality to movement. We tested for this possibility by a performing a chemotaxis assay on wild-type animals towards or away from ethanol. Ethanol has been previously reported to have mild to negative effects on chemotaxis only at very high concentrations (Bargmann *et al.* 1993; Lee *et al.* 2009). We found that, in our hands, ethanol did not act as either a chemoattractant or repellent whereas butanol, a longer chain alcohol, did act as a strong attractant (Figure S2A) as has been previously described (Bargmann *et al.* 1993). As an alternative approach, we adapted an osmotic aversion assay (Solomon *et al.* 2004) to investigate whether populations of worms would be averse to crossing a ring of ethanol. We found that if the ethanol concentration of the ring was increased to 100%, we could induce avoidance in comparison to a neutral (distilled water) control; however, 17 mM (0.1%) ethanol had no effect (Figure S2B). In contrast, worms were averse to octanol at concentrations as low as 1%.

We next investigated whether the low concentration of external ethanol was instead activating the IL2 chemosensory neurons to stimulate nematode motility through a G-protein coupled receptor (GPCR) dependent signalling mechanism. Physiological effects of ethanol are known to be modulated by various GPCRs, for example the $GABA_B$ or G-protein coupled corticotropin-releasing factor (CRH) 1 receptors (Nie *et al.* 2004; Kelm *et al.* 2011; Agabio and Colombo 2014). To screen GPCRs directly, however, would be prohibitively difficult as there are >1000 GPCRs in the *C. elegans* genome, very few of which have been functionally characterised (Frooninckx *et al.* 2012). For simplicity, therefore, we instead tested available G-protein mutants. Many *loss-of-function* nematode G-protein mutants are lethal or have severe locomotor defects, which would interfere with quantification using our assay.

Therefore, we screened *gain-of-function* mutants instead and determined that the stimulatory effect of 17 mM external ethanol remained intact for both $G_{\alpha o}$ (*goa-1*) and $G_{\alpha q}$ (*egl-30*) mutants, but was absent specifically for mutants of $G_{\alpha s}$, *gsa-1(ce81)* and *gsa-1(ce94)* (Figure 4A).

$G_{\alpha s}$ is a G-protein that, upon activation, stimulates adenylyl cyclase to synthesise the cAMP signalling molecule from ATP (Dorsam and Gutkind 2007). We addressed whether we could replicate the stimulatory effect of 17 mM ethanol by applying the chemical forskolin, which directly activates adenylyl cyclase pharmacologically. A dose-response curve of varying forskolin concentrations demonstrated that the stimulatory ethanol phenotype could indeed be phenocopied by forskolin (Figure 4B). Addition of ethanol and forskolin together did not have additive effects on nematode motility (Figure 4C) suggestive that ethanol and forskolin acted in the same pathway. One downstream cellular effector for cAMP is the cAMP-dependent protein kinase (PKA) and we tested for its role in the stimulatory ethanol phenotype by the addition of the specific PKA inhibitor H-89. On its own, H-89 had no effect on locomotion; however, it could completely block the stimulatory effects of ethanol and forskolin, either separately or both together (Figure 4C).

Next, as previously was shown for the stimulatory effects of ethanol, we verified that stimulation by forskolin was also dependent upon IL2-neuron expression of HSF-1 and HSP-16.48. In comparison to Bristol N2 wild-types, the effect of forskolin was absent in *hsf-1(sy441)* mutants, but was completely restored in both the full ($P_{hsf-1}::hsf-1$) or IL2 neuron-specific transgenic rescues ($P_{klp-6}::hsf-1$) (Figure 4D). Complementary to these results, stimulation by forskolin was blocked by the *hsf-1* inhibitor *hsb-1* expressed either pan-neuronally ($P_{rab-3}::hsb-1$) or in IL2 neurons specifically ($P_{klp-6}::hsb-1$) in Bristol N2 worms. As seen with ethanol, the effect of forskolin was restored in the OG532 single-copy rescue of *hsf-1(sy441)*, but not in the OG580 DNA-binding defective rescue (Figure S1). The forskolin

effect was also blocked in the $G_{\alpha s}$ *gain-of-function* mutants, *gsa-1(ce81)* and *gsa-1(ce94)*
(Figure 4D). Furthermore, pan-neuronal (P_{rab-3}::*hsp-16.48*) or IL2 specific (P_{klp-6}::*hsp-16.48*)
overexpression of *hsp-16.48* alone could completely rescue the forskolin phenotype of the
hsf-1(sy441) mutation (Figure 4E). Also identical to that seen with ethanol, overexpression
of *hsp-16.48* in Bristol N2 controls (P_{rab-3}::*hsp-16.48*) enhanced the effect of forskolin
whereas the N-terminal truncation mutant (P_{rab-3}::*hsp-16.48 Δ38-44*) appeared to act
negatively (Figure 4F). The truncation mutant again had no additional negative effects when
expressed in the *hsf-1(sy441)* background (Figure 4E). Taken together, these data indicate
that both the 17 mM ethanol and forskolin stimulatory phenotypes are likely acting through
the same pathway. Therefore, ethanol appears to activate a $G_{\alpha s}$-cAMP-PKA signalling
pathway that requires *hsf-1* and *hsp-16.48* expression within the IL2 neurons. Additionally,
the requirement of HSF-1/HSP-16.48 is likely to be acting downstream of adenylyl cyclase
activation as the effect of forskolin is absent in the *hsf-1(sy441)* mutant.

The data thus far pointed to an activation of $G_{\alpha s}$ in IL2 neurons by 17 mM external
ethanol; however, our evidence was obtained by pharmacological activation of the entire
nematode. We next wanted to activate $G_{\alpha s}$ in the IL2 neurons directly. To accomplish this
we expressed genetically a photoactivatable $G_{\alpha s}$-linked jellyfish opsin, JellyOp (Bailes *et al.*
2012), in the IL2 neurons specifically and demonstrated that photoactivation could enhance
the nematode locomotion rate to a level statistically indistinguishable from ethanol exposure
(Figure 5). In contrast, control worms demonstrated no enhancement of locomotion by
photostimulation; however, their ethanol effect remained intact. Importantly, photoactivation
of the $G_{\alpha s}$-linked JellyOp with the addition of ethanol did not produce an even greater
summative effect on locomotion rate supporting the hypothesis that the $G_{\alpha s}$-linked JellyOp
and ethanol were acting in the same pathway (Figure 5). Next we antagonised $G_{\alpha s}$ signalling
in IL2 neurons specifically by genetic expression of a photoactivatable $G_{\alpha i}$-linked human rod

opsin (hRh1) (Cao *et al.* 2012; Bailes and Lucas 2013) which acts to counter $G_{\alpha s}$ by inhibiting the production of cAMP. On its own, photoactivation of the $G_{\alpha i}$-linked hRh1 again had no effect on nematode locomotion; however, it was able to block completely the stimulatory effect of low concentrations of external ethanol (Figure 5). As an alternative approach to optogenetic activation or inhibition of the $G_{\alpha s}$ signalling pathway, we produced a transgenic worm with IL2 neuron-specific RNAi against the catalytic subunit of *C. elegans* PKA ($P_{klp-6}::kin-1::P_{klp-6}$). The created transgenic worms appeared qualitatively normal and had only a small quantitative reduction in basal locomotion rate (Table S1). Whilst we cannot quantify definitive cell-specificity of the RNAi, if the PKA knockdown had spread greatly to other cells it would be expected to be lethal (Rual *et al.* 2004). Therefore we are reasonably confident in a degree of cellular restriction of the knockdown. Despite the qualitatively wild-type appearance of the worms, the stimulation of locomotion by either ethanol or forskolin was absent (Figure S3). These data support the interpretation that the effects of ethanol to stimulate *C. elegans* locomotion are regulated in IL2 neurons by a $G_{\alpha s}$ signalling pathway.

Finally we were interested in identifying what was potentially acting downstream of the $G_{\alpha s}$-cAMP-PKA signalling pathway. PKA is a serine-threonine kinase that would be expected to phosphorylate many downstream targets in response to activation. Sec1-Munc18 (SM) proteins are essential components of the exocytotic machinery thought to function primarily through interactions with soluble N-ethylmaleimide sensitive factor receptor (SNARE) proteins (Rizo and Sudhof 2012). We have previously shown that expression of a single point mutation in the *C. elegans* SM protein UNC-18 (D214N) was also able to block the low ethanol phenotype (Graham *et al.* 2009). We therefore suspected UNC-18 could be one potential downstream target for PKA phosphorylation. Both mammalian Munc18 and the nematode orthologue UNC-18 are known to be phosphorylated by Protein Kinase C

(Barclay *et al.* 2003; Edwards *et al.* 2012); however, PKA phosphorylation has not been

previously demonstrated. We expressed recombinant UNC-18 and exposed it to PKA,

determining that it could be phosphorylated *in vitro* (Figure 6A). We then determined *in*

vitro phosphorylation sites for PKA by mass spectrometry, positively identifying Ser322 as

an *in vitro* PKA target (Figure 6B). We tested the relevance of this putative phosphorylation

site *in vivo* by expressing phospho-null versions of UNC-18 (S322A) which act in a dominant

fashion to endogenous *unc-18* (Edwards *et al.* 2012). In our assays, expression of this single

point mutation of UNC-18 pan-neuronally (P_{unc-18}::*unc-18 S322A*) or in IL2 neurons

specifically (P_{klp-6}::*unc-18 S322A*) was able to block completely the stimulatory effects on

motility of either ethanol or forskolin (Figure 6C, D).

Discussion

In this manuscript we demonstrate that a $G_{\alpha s}$-signalling pathway is stimulated by the addition of ethanol at external concentrations (17 mM; 0.1%) whose absolute values are physiologically consistent with blood alcohol limits for impaired driving. Through a combination of genetics, pharmacology and optogenetic manipulation, we have uniquely delineated the entire cell signalling pathway in response to ethanol in IL2 chemosensory neurons specifically (Figure 7). Our model for ethanol stimulation is that ethanol, in some way, activates $G_{\alpha s}$ to stimulate adenylyl cyclase to produce cAMP. The cAMP in turn activates PKA to phosphorylate various downstream proteins, one possibility of which is the synaptic SM protein UNC-18. The ultimate downstream effect of this cellular signalling pathway is an enhancement in nematode locomotion, as quantified by thrashing rate. This cell-specific signalling pathway requires the transcription factor HSF-1, most likely through its transcriptional control of the α-crystallin orthologue, small heat shock protein HSP-16.48.

Our data support the interpretation that a $G_{\alpha s}$-signalling pathway is directly activated or modulated by ethanol. There is ample evidence in other systems for ethanol-induced activation of G protein coupled signalling pathways, at least *in vitro*. Ethanol can enhance GABA release and the extent of this enhancement can be regulated by various GPCRs, mostly via $G_{\alpha i}$-coupled receptors (Kelm et al. 2011). Ethanol activation of GABAergic release in the central amygdala, an area of the brain prominently associated with alcohol dependence, requires the G-protein coupled corticotropin-releasing factor (CRH) 1 receptor (Nie *et al.* 2004). Downstream of GPCRs, ethanol can activate directly specific forms of adenylyl cyclase (Yoshimura and Tabakoff 1995; Yoshimura *et al.* 2006), affect cellular cAMP levels (Rex *et al.* 2008; Gupta *et al.* 2013), activate PKA (Kelm *et al.* 2008; Wang *et al.* 2015) and induce protein phosphorylation (Conti *et al.* 2009). Genetic or pharmacological manipulation of individual components of this pathway has measurable effects on complex

alcohol dependency phenotypes as adenylyl cyclase mutants and knockouts affect ethanol

sensitivities and consumption in both mice and *Drosophila* (Moore *et al.* 1998; Maas *et al.*

2005; Xu *et al.* 2012). Indeed the role of cAMP in the ethanol-induced stimulation of

locomotion of mice was recently reported using a selective phosphodiesterase-4 inhibitor

(Balino *et al.* 2016). Despite evidence of the $G_{\alpha s}$-signalling pathway in other models, it has

been relatively unexplored in *C. elegans*. In *C. elegans*, the CRH1 homogue *seb-3* has a

characterised high alcohol phenotype; however, *seb-3* is expressed in head ganglia and nerve

cords (Jee et al. 2013) and not sensory neurons such as the IL2 neurons specifically. Our data

use combinations of optogenetic, genetic and pharmacological manipulation to trace the

involvement of the entire $G_{\alpha s}$ -cAMP-PKA signalling pathway in the IL2 neurons in ethanol-

dependent stimulation. Additionally we extend this pathway to the downstream

phosphorylation of the exocytotic protein UNC-18 and implicate HSP-16.48 as a novel

regulatory protein.

Phosphorylation of synaptic proteins is a dynamic mechanism for the regulation of

vesicle fusion and synaptic transmission. Many phosphorylation targets have been described

for serine/threonine kinases, although mostly *in vitro*. Phosphorylation of Munc18 has been

demonstrated *in vivo*, primarily by Protein Kinase C (De Vries *et al.* 2000; Craig *et al.* 2003).

PKA has not previously been shown to phosphorylate Munc18 or UNC-18, despite strong

evidence that it does phosphorylate other synaptic proteins such as cysteine string protein

(Evans *et al.* 2001). Both protein kinase C and PKA phosphorylation consensus sequences

have similar requirements of basic amino acids upstream of the target serine and indeed the

region upstream of Ser322 is rich in lysine residues (Edwards *et al.* 2012). In rat pancreatic

acini, intriguingly, PKC-dependent phosphorylation of Munc18C occurs in response to acute

exposure to ethanol (Cosen-Binker *et al.* 2007). Physiologically, phosphorylation alters the

kinetics of amperometric spikes, in particular reducing the quantal size of individual release

events (Barclay *et al.* 2003). Munc18 phosphorylation contributes to short-term plasticity at the synapse, by controlling post-tetanic potentiation (Genc *et al.* 2014) and UNC-18 phosphorylation contributes to thermosensory behaviours of *C. elegans* (Edwards *et al.* 2012). Biochemically, phosphorylation of this region of either UNC-18 or Munc18 reduces the binding affinity for closed-conformation syntaxin (Barclay *et al.* 2003; Edwards *et al.* 2012). The classically characterised closed-conformation mutation of Munc18, R39C, however has no effect on the stimulatory alcohol phenotype (Johnson *et al.* 2013) arguing against the physiological effects of low ethanol concentrations being achieved through regulation of that particular interaction. The IL2 neurons release acetylcholine as a fast neurotransmitter (Lee *et al.* 2012) and connect into the main locomotor circuits via intermediary neurons (White *et al.* 1986). It is therefore possible that phosphorylation is altering synaptic vesicle fusion in the IL2 neurons thereby shaping the patterns of electrical activity governing nematode motility.

Our data demonstrate that the α-crystallin orthologue HSP-16.48 acts directly downstream of HSF-1 indicating that the effects of HSF-1 in this phenotype are likely simply as a transcription factor driving constitutive HSP-16.48 expression. HSF-1 controls the expression of heat-inducible stress proteins such as the small HSPs, and HSP-16.48 specifically, as evidenced by numerous experiments (Hsu *et al.* 2003; Prahlad *et al.* 2008; Larance *et al.* 2011; Kourtis *et al.* 2012). Exposure to very high concentrations of ethanol can induce the expression of many heat shock proteins (Kwon *et al.* 2004; Pignataro *et al.* 2007; Urquhart *et al.* 2016) and overexpression of some HSPs can alter sensitivity to the sedative effects of ethanol (Awofala *et al.* 2011). In *C. elegans*, basal expression of *hsp-16.48* alters the sedative effects of high doses of ethanol, but its overexpression only partially rescues the *hsf-1(sy441)* mutant phenotype (Johnson *et al.* 2016). In contrast, our results indicate that *hsp-16.48* can completely restore the stimulatory phenotype for the *hsf-1(sy441)*

mutant. Although there is little constitutive HSP-16.48 expressed, even in response to 400 mM ethanol, our RNAi experiments show that these small quantities are sufficient to affect whole animal behaviour. Small HSPs can be directly phosphorylated by PKA (Garrido *et al.* 2012), but it is currently unknown how HSP-16.48 regulates the $G_{\alpha s}$ -cAMP-PKA signalling pathway. It may be that HSP-16.48 is acting simply as a chaperone to preserve either structural conformation of individual proteins, protein-protein interactions or possibly to assist in the phosphorylation event itself. Alternatively, HSP-16.48 may directly interact with specific components of the signalling pathway independent of its chaperone ability. Nonetheless, the correct functioning of HSP-16.48 in ethanol-dependent phenotypes explicitly required a 7 amino acid region of the protein's N-terminus, a region not found in other small HSPs linked to temperature stress tolerance (Kourtis *et al.* 2012) and it will be intriguing to determine the mechanistic role for this protein region.

Our experiments have used thrashing as a measure of locomotion (Gjorgjieva *et al.* 2014). The main rationale for this selection was the simplicity and reproducibility of the assay. It is unknown experimentally whether other measures of locomotion, such as body bends or locomotor speed, would be similarly affected; however, that speculation would be considered likely. High alcohol concentrations reduce all aspects of locomotion by similar extents including thrashing (Mitchell *et al.* 2007; Graham *et al.* 2009; Johnson *et al.* 2013), body bends (Johnson *et al.* 2016) and locomotor speed (Davies *et al.* 2003; Kapfhamer *et al.* 2008) and there is no reason to suspect differences with low alcohol concentrations. Exposure to high or low ethanol has no reported effect on reversals or omega turns of *C. elegans* on agar (Mitchell *et al.* 2010), but high alcohol did increase spontaneous reversals in solution by ~1 reversal per minute (Topper *et al.* 2014). Whilst uncharacterised in this study, it is unlikely that a change in reversal frequency would be significant enough to influence rates as high as 110-120 thrashes per minute.

The internal concentration of ethanol in nematodes is reported to be approximately 10% of external experimental levels due to poor penetration through the cuticle (Davies *et al.* 2003; Alaimo *et al.* 2012; Johnson *et al.* 2016). The structure of the IL2 neurons however, with dendritic projections directly to the exterior of the body (White *et al.* 1986), would be in contact with the exact level of ethanol seen in solution. Therefore, it is unclear whether this low alcohol phenotype represents a phenotypic response to 17 mM or a substantially reduced concentration. In either case, however, this phenotype does indicate a neuronal cell signalling effect in *C. elegans* to ethanol at levels that would be seen in intoxicated humans. The stimulation of locomotion has been reproducibly demonstrated in *C. elegans* (Graham *et al.* 2009; Johnson *et al.* 2013) but is smaller than that seen in *Drosophila* (Wolf et al. 2002). It is difficult to determine whether there could be a further enhancement of locomotion with exposure to higher levels of ethanol as competing depressive and stimulatory effects of ethanol may begin to cancel each other out as concentration is increased. Indeed, there is no net effect of 100 mM external ethanol on locomotion rate (Davies *et al.* 2003; Mitchell *et al.* 2007; Graham *et al.* 2009; Johnson *et al.* 2016). It remains possible that the stimulatory effects of 17 mM ethanol are actually underrepresented here due to the antagonistic sedative effects of higher alcohol concentrations. Why would *C. elegans* increase their movement in response to 17 mM ethanol? The ecology of the species is not fully understood; however, some evidence point to *C. elegans* feeding on bacteria associated with decomposing material. Unlike longer chain alcohols, however, evidence for ethanol acting as a chemotactic cue signalling a potential nutrient source is not well supported. Although we were unable to reproduce the results, some data point to ethanol acting as a low level chemorepellant (Bargmann *et al.* 1993; Lee *et al.* 2009). It is therefore conceivable that the stimulus in locomotor rate is enhancing escape or avoidance of a potentially poisonous substance. Alternatively, the locomotor stimulus is merely reflective of an indirect activation of a

neuronal G-protein signalling pathway that feeds into the circuitry governing nematode locomotion (Gjorgjieva *et al.* 2014).

Alcohol acts paradoxically as both a depressant and as a stimulant. These stimulatory effects in humans are thought to be more rewarding than sedative effects and thus may play a more prominent role in determining addiction. The differentiator model for risk to alcoholism is associated with a trade-off between stimulant and sedative effects (Hendler *et al.* 2013). We have shown a unique genetic link between the α-crystallin homologue HSP-16.48 and both the sedative (Johnson *et al.* 2016) and now also the stimulatory effects of alcohol where an increase in HSP-16.48 expression biphasically both enhances ethanol-induced stimulation and decreases ethanol-induced sedation. Importantly, the expression of the α-crystallin chaperone is upregulated in mice strains with a high alcohol intake preference (Mulligan *et al.* 2006) as well as human alcohol addicts (Iwamoto *et al.* 2004) indicative that the phenotypic effects presented here may indeed reflect neuronal pathways and have biomedical relevance in higher organisms. This identification of an ethanol-dependent signalling pathway, from G-protein to the phosphorylation target of UNC-18, therefore presents novel targets for future pharmacological intervention that could be exploited to control the devastating physiological effects of alcohol.

Acknowledgements

Literature Cited

Agabio, R., and G. Colombo, 2014 GABAB receptor ligands for the treatment of alcohol use disorder: preclinical and clinical evidence. Front Neurosci 8**:** 140.

Alaimo, J. T., S. J. Davis, S. S. Song, C. R. Burnette, M. Grotewiel *et al.*, 2012 Ethanol metabolism and osmolarity modify behavioral responses to ethanol in C. elegans. Alcohol Clin Exp Res 36**:** 1840-1850.

Anckar, J., and L. Sistonen, 2011 Regulation of HSF1 function in the heat stress response: implications in aging and disease. Annu. Rev. Biochem. 80**:** 1089-1115.

Awofala, A. A., S. Jones and J. A. Davies, 2011 The *Heat Shock Protein 26* Gene is Required for Ethanol Tolerance in *Drosophila*. J. Exp. Neurosci. 5**:** 31-44.

Bailes, H. J., and R. J. Lucas, 2013 Human melanopsin forms a pigment maximally sensitive to blue light (lambdamax approximately 479 nm) supporting activation of G(q/11) and G(i/o) signalling cascades. Proc Biol Sci 280**:** 20122987.

Bailes, H. J., L. Y. Zhuang and R. J. Lucas, 2012 Reproducible and sustained regulation of Galphas signalling using a metazoan opsin as an optogenetic tool. PLoS ONE 7**:** e30774.

Baird, N. A., P. M. Douglas, M. S. Simic, A. R. Grant, J. J. Moresco *et al.*, 2014 HSF-1-mediated cytoskeletal integrity determines thermotolerance and life span. Science 346**:** 360-363.

Balino, P., J. C. Ledesma and C. M. Aragon, 2016 Role of phosphodiesterase-4 on ethanol elicited locomotion and narcosis. Neuropharmacology 101**:** 271-278.

Barclay, J. W., T. J. Craig, R. J. Fisher, L. F. Ciufo, G. J. Evans *et al.*, 2003 Phosphorylation of Munc18 by protein kinase C regulates the kinetics of exocytosis. J. Biol. Chem. 278**:** 10538-10545.

Barclay, J. W., M. E. Graham, M. R. Edwards, J. R. Johnson, A. Morgan *et al.*, 2010 Presynaptic targets for acute ethanol sensitivity. Biochem Soc Trans 38**:** 172-176.

Bargmann, C. I., E. Hartwieg and H. R. Horvitz, 1993 Odorant-selective genes and neurons mediate olfaction in C. elegans. Cell 74**:** 515-527.

Bettinger, J. C., and A. G. Davies, 2014 The role of the BK channel in ethanol response behaviors: evidence from model organism and human studies. Front Physiol 5**:** 346.

Bhandari, P., J. S. Hill, S. P. Farris, B. Costin, I. Martin *et al.*, 2012 Chloride intracellular channels modulate acute ethanol behaviors in Drosophila, Caenorhabditis elegans and mice. Genes Brain Behav 11**:** 387-397.

Brenner, S., 1974 The genetics of caenorhabditis elegans. Genetics 77**:** 71-94.

Burket, C. T., C. E. Higgins, L. C. Hull, P. M. Berninsone and E. F. Ryder, 2006 The C. elegans gene dig-1 encodes a giant member of the immunoglobulin superfamily that promotes fasciculation of neuronal processes. Dev Biol 299**:** 193-205.

Cao, P., W. Sun, K. Kramp, M. Zheng, D. Salom *et al.*, 2012 Light-sensitive coupling of rhodopsin and melanopsin to G(i/o) and G(q) signal transduction in Caenorhabditis elegans. Faseb J 26**:** 480-491.

Conti, A. C., J. W. Maas, Jr., K. L. Moulder, X. Jiang, B. A. Dave *et al.*, 2009 Adenylyl cyclases 1 and 8 initiate a presynaptic homeostatic response to ethanol treatment. PLoS ONE 4**:** e5697.

Cosen-Binker, L. I., P. P. Lam, M. G. Binker, J. Reeve, S. Pandol *et al.*, 2007 Alcohol/cholecystokinin-evoked pancreatic acinar basolateral exocytosis is mediated by protein kinase C alpha phosphorylation of Munc18c. J Biol Chem 282**:** 13047-13058.

Craig, T. J., G. J. O. Evans and A. Morgan, 2003 Physiological regulation of Munc18/nSec1 phosphorylation on serine-313. J. Neurochem. 86**:** 1450-1457.

Davies, A. G., J. T. Pierce-Shimomura, H. Kim, M. K. VanHoven, T. R. Thiele *et al.*, 2003 A central role of the BK potassium channel in behavioral responses to ethanol in *C. elegans*. Cell 115**:** 655-666.

de Vries, K. J., A. Geijtenbeek, E. C. Brian, P. N. E. de Graan, W. Ghijsen *et al.*, 2000 Dynamics of munc18-1 phosphorylation/dephosphorylation in rat brain nerve terminals. Eur. J. Neurosci. 12**:** 385-390.

Devineni, A. V., and U. Heberlein, 2013 The evolution of Drosophila melanogaster as a model for alcohol research. Annu Rev Neurosci 36**:** 121-138.

Dorsam, R. T., and J. S. Gutkind, 2007 G-protein-coupled receptors and cancer. Nat Rev Cancer 7**:** 79-94.

Edwards, M. R., J. R. Johnson, K. Rankin, R. E. Jenkins, C. Maguire *et al.*, 2012 PKC-2 phosphorylation of UNC-18 Ser322 in AFD neurons regulates temperature dependency of locomotion. J. Neurosci. 32**:** 7042-7051.

Esposito, G., E. Di Schiavi, C. Bergamasco and P. Bazzicalupo, 2007 Efficient and cell specific knock-down of gene function in targeted C. elegans neurons. Gene 395**:** 170-176.

Evans, G. J. O., M. C. Wilkinson, M. E. Graham, K. M. Turner, L. H. Chamberlain *et al.*, 2001 Phosphorylation of cysteine string protein by PKA: implications for the modulation of exocytosis. J. Biol. Chem. 276**:** 47877-47885.

Frooninckx, L., L. Van Rompay, L. Temmerman, E. Van Sinay, I. Beets *et al.*, 2012 Neuropeptide GPCRs in C. elegans. Front Endocrinol (Lausanne) 3**:** 167.

Garrido, C., C. Paul, R. Seigneuric and H. H. Kampinga, 2012 The small heat shock proteins family: the long forgotten chaperones. Int J Biochem Cell Biol 44**:** 1588-1592.

Genc, O., O. Kochubey, R. F. Toonen, M. Verhage and R. Schneggenburger, 2014 Munc18-1 is a dynamically regulated PKC target during short-term enhancement of transmitter release. Elife 3**:** e01715.

Gengyo-Ando, K., H. Kitayama, M. Mukaida and Y. Ikawa, 1996 A murine neural specific homolog corrects cholinergic defects in Caenorhabditis elegans unc-18 mutants. J.Neurosci. 16**:** 6695-6702.

Gjorgjieva, J., D. Biron and G. Haspel, 2014 Neurobiology of Caenorhabditis elegans Locomotion: Where Do We Stand? Bioscience 64**:** 476-486.

Graham, M. E., M. R. Edwards, L. Holden-Dye, A. Morgan, R. D. Burgoyne *et al.*, 2009 UNC-18 Modulates Ethanol Sensitivity in Caenorhabditis elegans. Mol. Biol. Cell 20**:** 43-55.

Gupta, R., E. Qualls-Creekmore and M. Yoshimura, 2013 Real-time monitoring of intracellular cAMP during acute ethanol exposure. Alcohol Clin Exp Res 37**:** 1456-1465.

Hajdu-Cronin, Y. M., W. J. Chen and P. W. Sternberg, 2004 The L-type cyclin CYL-1 and the heat-shock-factor HSF-1 are required for heat-shock-induced protein expression in *Caenorhabditis elegans*. Genetics 168**:** 1937-1949.

Harris, R. A., J. R. Trudell and S. J. Mihic, 2008 Ethanol's molecular targets. Sci Signal 1**:** re7.

Hendler, R. A., V. A. Ramchandani, J. Gilman and D. W. Hommer, 2013 Stimulant and sedative effects of alcohol. Curr Top Behav Neurosci 13**:** 489-509.

House of Commons Transport Committee, 2010 Drink and drug driving law: First report of session 2010-2011. https://publications.parliament.uk/pa/cm201011/cmselect/cmtran/460/460.pdf.

Howard, R. J., P. A. Slesinger, D. L. Davies, J. Das, J. R. Trudell *et al.*, 2011 Alcohol-binding sites in distinct brain proteins: the quest for atomic level resolution. Alcohol Clin. Exp. Res. 35**:** 1561-1573.

Howard, R. J., J. R. Trudell and R. A. Harris, 2014 Seeking structural specificity: direct modulation of pentameric ligand-gated ion channels by alcohols and general anesthetics. Pharmacol Rev 66**:** 396-412.

Hsu, A.-L., C. T. Murphy and C. Kenyon, 2003 Regulation of aging and age-related disease by DAF-16 and heat-shock factor. Science 300**:** 1142-1145.

Husson, S. J., A. Gottschalk and A. M. Leifer, 2013 Optogenetic manipulation of neural activity in C. elegans: from synapse to circuits and behaviour. Biol Cell 105**:** 235-250.

Iwamoto, K., M. Bundo, M. Yamamoto, H. Ozawa, T. Saito *et al.*, 2004 Decreased expression of NEFH and PCP4/PEP19 in the prefrontal cortex of alcoholics. Neurosci Res 49**:** 379-385.

Johnson, J. R., S. Kashyap, K. Rankin and J. W. Barclay, 2013 Rab-3 and unc-18 interactions in alcohol sensitivity are distinct from synaptic transmission. PLoS ONE 8**:** e81117.

Johnson, J. R., D. Rajamanoharan, H. V. McCue, K. Rankin and J. W. Barclay, 2016 Small Heat Shock Proteins Are Novel Common Determinants of Alcohol and Nicotine Sensitivity in Caenorhabditis elegans. Genetics 202**:** 1013-1027.

Kamath, R. S., and J. Ahringer, 2003 Genome-wide RNAi screening in Caenorhabditis elegans. Methods 30**:** 313-321.

Kampinga, H. H., and E. A. Craig, 2010 The HSP70 chaperone machinery: J proteins as drivers of functional specificity. Nat. Rev. Mol. Cell Biol. 11**:** 579-592.

Kapfhamer, D., J. C. Bettinger, A. G. Davies, C. L. Eastman, E. A. Smail *et al.*, 2008 Loss of RAB-3/A in C. elegans and the mouse affects behavioral response to ethanol. Genes Brain Behav. 7**:** 669-676.

Kashyap, S. S., J. R. Johnson, H. V. McCue, X. Chen, M. J. Edmonds *et al.*, 2014 Caenorhabditis elegans dnj-14, the orthologue of the DNAJC5 gene mutated in adult onset neuronal ceroid lipofuscinosis, provides a new platform for neuroprotective drug screening and identifies a SIR-2.1-independent action of resveratrol. Hum Mol Genet 23**:** 5916-5927.

Kaun, K. R., A. V. Devineni and U. Heberlein, 2012 Drosophila melanogaster as a model to study drug addiction. Hum. Genet. 131**:** 959-975.

Kelm, M. K., H. E. Criswell and G. R. Breese, 2008 The role of protein kinase A in the ethanol-induced increase in spontaneous GABA release onto cerebellar Purkinje neurons. J Neurophysiol 100**:** 3417-3428.

Kelm, M. K., H. E. Criswell and G. R. Breese, 2011 Ethanol-enhanced GABA release: a focus on G protein-coupled receptors. Brain Res Rev 65**:** 113-123.

Kondo, N., M. Katsuno, H. Adachi, M. Minamiyama, H. Doi *et al.*, 2013 Heat shock factor-1 influences pathological lesion distribution of polyglutamine-induced neurodegeneration. Nat Commun 4**:** 1405.

Kourtis, N., V. Nikoletopoulou and N. Tavernarakis, 2012 Small heat-shock proteins protect from heat-stroke-associated neurodegeneration. Nature 490**:** 213-218.

Kwon, J. Y., M. Hong, M. S. Choi, S. Kang, K. Duke *et al.*, 2004 Ethanol-response genes and their regulation analyzed by a microarray and comparative approach in the nematode *Caenorhabditis elegans*. Genomics 83**:** 600-614.

Larance, M., A. P. Bailly, E. Pourkarimi, R. T. Hay, G. Buchanan *et al.*, 2011 Stable-isotope labeling with amino acids in nematodes. Nat Methods 8**:** 849-851.

Lee, H., M. K. Choi, D. Lee, H. S. Kim, H. Hwang *et al.*, 2012 Nictation, a dispersal behavior of the nematode Caenorhabditis elegans, is regulated by IL2 neurons. Nat Neurosci 15**:** 107-112.

Lee, J., C. Jee and S. L. McIntire, 2009 Ethanol preference in C. elegans. Genes Brain Behav 8**:** 578-585.

Maas, J. W., Jr., R. A. Indacochea, L. M. Muglia, T. T. Tran, S. K. Vogt *et al.*, 2005 Calcium-stimulated adenylyl cyclases modulate ethanol-induced neurodegeneration in the neonatal brain. J Neurosci 25**:** 2376-2385.

Mello, C. C., J. M. Kramer, D. Stinchcomb and V. Ambros, 1991 Efficient gene transfer in C.elegans: extrachromosomal maintenance and integration of transforming sequences. Embo J 10**:** 3959-3970.

Mendillo, M. L., S. Santagata, M. Koeva, G. W. Bell, R. Hu *et al.*, 2012 HSF1 drives a transcriptional program distinct from heat shock to support highly malignant human cancers. Cell 150**:** 549-562.

Mitchell, P., R. Mould, J. Dillon, S. Glautier, I. Andrianakis *et al.*, 2010 A differential role for neuropeptides in acute and chronic adaptive responses to alcohol: behavioural and genetic analysis in Caenorhabditis elegans. PLoS One 5**:** e10422.

Mitchell, P. H., K. Bull, S. Glautier, N. A. Hopper, L. Holden-Dye *et al.*, 2007 The concentration-dependent effects of ethanol on Caenorhabditis elegans behaviour. Pharmacogenomics J 7**:** 411-417.

Moore, M. S., J. DeZazzo, A. Y. Luk, T. Tully, C. M. Singh *et al.*, 1998 Ethanol intoxication in Drosophila: Genetic and pharmacological evidence for regulation by the cAMP signaling pathway. Cell 93**:** 997-1007.

Morimoto, R. I., 2011 The heat shock response: systems biology of proteotoxic stress in aging and disease. Cold Spring Harb Symp Quant Biol 76**:** 91-99.

Morton, E. A., and T. Lamitina, 2013 Caenorhabditis elegans HSF-1 is an essential nuclear protein that forms stress granule-like structures following heat shock. Aging Cell 12**:** 112-120.

Mulligan, M. K., I. Ponomarev, R. J. Hitzemann, J. K. Belknap, B. Tabakoff *et al.*, 2006 Toward understanding the genetics of alcohol drinking through transcriptome meta-analysis. Proc Natl Acad Sci U S A 103**:** 6368-6373.

Nie, Z., P. Schweitzer, A. J. Roberts, S. G. Madamba, S. D. Moore *et al.*, 2004 Ethanol augments GABAergic transmission in the central amygdala via CRF1 receptors. Science 303**:** 1512-1514.

Olsen, R. W., G. D. Li, M. Wallner, J. R. Trudell, E. J. Bertaccini *et al.*, 2014 Structural models of ligand-gated ion channels: sites of action for anesthetics and ethanol. Alcohol Clin Exp Res 38**:** 595-603.

Peden, E. M., and M. M. Barr, 2005 The KLP-6 kinesin is required for male mating behaviors and polycystin localization in Caenorhabditis elegans. Curr Biol 15**:** 394-404.

Phillips, T. J., and E. H. Shen, 1996 Neurochemical bases of locomotion and ethanol stimulant effects. Int Rev Neurobiol 39**:** 243-282.

Pignataro, L., A. N. Miller, L. Ma, S. Midha, P. Protiva *et al.*, 2007 Alcohol regulates gene expression in neurons via activation of heat shock factor 1. J Neurosci 27**:** 12957-12966.

Prahlad, V., T. Cornelius and R. I. Morimoto, 2008 Regulation of the cellular heat shock response in Caenorhabditis elegans by thermosensory neurons. Science 320**:** 811-814.

Rex, E. B., M. L. Rankin, M. A. Ariano and D. R. Sibley, 2008 Ethanol regulation of D(1) dopamine receptor signaling is mediated by protein kinase C in an isozyme-specific manner. Neuropsychopharmacology 33**:** 2900-2911.

Rizo, J., and T. C. Sudhof, 2012 The membrane fusion enigma: SNAREs, Sec1/Munc18 proteins, and their accomplices--guilty as charged? Annu Rev Cell Dev Biol 28**:** 279-308.

Rual, J. F., J. Ceron, J. Koreth, T. Hao, A. S. Nicot *et al.*, 2004 Toward improving Caenorhabditis elegans phenome mapping with an ORFeome-based RNAi library. Genome Res 14**:** 2162-2168.

Satyal, S. H., D. Chen, S. G. Fox, J. M. Kramer and R. I. Morimoto, 1998 Negative regulation of the heat shock transcriptional response by HSBP1. Genes Dev 12**:** 1962-1974.

Solomon, A., S. Bandhakavi, S. Jabbar, R. Shah, G. J. Beitel *et al.*, 2004 Caenorhabditis elegans OSR-1 regulates behavioral and physiological responses to hyperosmotic environments. Genetics 167**:** 161-170.

Speca, D. J., D. Chihara, A. M. Ashique, M. S. Bowers, J. T. Pierce-Shimomura *et al.*, 2010 Conserved role of unc-79 in ethanol responses in lightweight mutant mice. PLoS Genet 6.

Topper, S. M., S. C. Aguilar, V. Y. Topper, E. Elbel and J. T. Pierce-Shimomura, 2014 Alcohol disinhibition of behaviors in C. elegans. PLoS ONE 9**:** e92965.

Trudell, J. R., R. O. Messing, J. Mayfield and R. A. Harris, 2014 Alcohol dependence: molecular and behavioral evidence. Trends Pharmacol Sci 35**:** 317-323.

Urquhart, K. R., Y. Zhao, J. A. Baker, Y. Lu, L. Yan *et al.*, 2016 A novel heat shock protein alpha 8 (Hspa8) molecular network mediating responses to stress- and ethanol-related behaviors. Neurogenetics 17**:** 91-105.

Vihervaara, A., and L. Sistonen, 2014 HSF1 at a glance. J Cell Sci 127**:** 261-266.

Wang, X., Z. Yang, Y. Sun, H. Zhou, G. Chu *et al.*, 2015 Ethanol Activation of PKA Mediates Single-Minded 2 Expression in Neuronal Cells. Mol Neurobiol 52**:** 1234-1244.

White, J. G., E. Southgate, J. N. Thomson and S. Brenner, 1986 The structure of the nervous system of the nematode Caenorhabditis elegans. Philos Trans R Soc Lond B Biol Sci 314**:** 1-340.

WHO, 2011 Global status report on alcohol and health. http://www.who.int/substance_abuse/publications/global_alcohol_report/en/index.html.

Wolf, F. W., A. R. Rodan, L. T. Tsai and U. Heberlein, 2002 High-resolution analysis of ethanol-induced locomotor stimulation in Drosophila. J Neurosci 22**:** 11035-11044.

Xu, S., T. Chan, V. Shah, S. Zhang, S. D. Pletcher *et al.*, 2012 The propensity for consuming ethanol in Drosophila requires rutabaga adenylyl cyclase expression within mushroom body neurons. Genes Brain Behav 11**:** 727-739.

Yoshimura, M., S. Pearson, Y. Kadota and C. E. Gonzalez, 2006 Identification of ethanol responsive domains of adenylyl cyclase. Alcohol Clin Exp Res 30**:** 1824-1832.

Yoshimura, M., and B. Tabakoff, 1995 Selective effects of ethanol on the generation of cAMP by particular members of the adenylyl cyclase family. Alcohol Clin Exp Res 19**:** 1435-1440.

Zhang, F., A. Bhattacharya, J. C. Nelson, N. Abe, P. Gordon *et al.*, 2014 The LIM and POU homeobox genes ttx-3 and unc-86 act as terminal selectors in distinct cholinergic and serotonergic neuron types. Development 141**:** 422-435.

Figure Legends

Figure 1. Low concentrations of ethanol stimulate *C. elegans* locomotion in an *hsf-1-*dependent fashion. **(A)** In comparison to untreated controls, exposure to 17 mM ethanol (+ethanol) significantly increased the locomotion of Bristol N2 wild-type worms. The *hsf-1(sy441) loss-of-function* mutant demonstrated a reduced untreated locomotion rate that was unaffected by ethanol. Locomotion rate was quantified by thrashing after 10 minutes immersion in Dent's solution. *; $P<0.001$ (one-way analysis of variance with Tukey post-hoc comparisons); n.s. = not significant. N = 100 for each condition. **(B)** The absence of ethanol stimulation in *hsf-1(sy441)* worms is independent of temperature. Locomotion rate was quantified at the indicated temperature and expressed here as a percentage of mean thrashing rate of untreated worms. At all temperatures, ethanol stimulated Bristol N2 locomotion, but had no effect on *hsf-1(sy441)* loss-of-function worms. *; $P<0.001$ (two-way analysis of variance with Tukey post-hoc comparisons); N = 20 for each condition.

Figure 2. The *hsf-1*-dependence of the low ethanol stimulation of locomotion requires *hsf-1* expression in IL2 neurons. **(A)** In *hsf-1(sy441)* worms, the low ethanol stimulation of locomotion was restored by transgenic rescue of wild-type *hsf-1* under the control of its endogenous (P_{hsf-1}), pan-neuronal (P_{rab-3}), cholinergic neuron (P_{unc-17}) or ciliated sensory neuron promoter (P_{osm-6}). Tissue-specific expression in muscle (P_{myo-3}), interneurons (P_{glr-1}) or the AFD thermosensory neurons (P_{gcy-8}) was unable to rescue the *hsf-1(sy441)* mutant. In Bristol N2 worms, overexpression of *hsf-1* under its endogenous promoter (P_{hsf-1}) had no additional effect on ethanol stimulation of locomotion whereas neuronal overexpression of the *hsf-1* inhibitor, *hsb-1*, blocked the ethanol effect. **(B)** Cartoon schematic of the *C. elegans* head region indicating the location of the IL2 neurons (1 neuron of each of the 3 pairs are depicted) and their projections (in red) adjacent to the pharynx (in green). The approximate anterior-posterior (A-P) and ventral-dorsal (V-D) axes are indicated and apply to

part C as well. **(C)** Expression of green fluorescent protein (GFP) under the control of the *klp*-6 promoter, showing expression in the IL2 neurons of *hsf-1(sy441)* mutants. Expression in Bristol N2 worms was anatomically similar. **(D)** In comparison to *hsf-1(sy441)* worms, low ethanol stimulation of locomotion was restored by transgenic expression of wild-type *hsf-1* using an IL2 specific promoter (P_{klp-6}). In Bristol N2 worms, IL2 neuron overexpression of the *hsf-1* inhibitor, *hsb-1*, blocked the ethanol effect. In both (A) and (D), data are expressed normalised to untreated controls. For each experiment, exposure to ethanol enhanced the locomotion rate of Bristol N2 worms (Mann-Whitney U-test; P<0.05). * indicates significant difference in comparison to treated Bristol N2. Comparisons were made by one-way analysis of variance with Tukey post-hoc comparisons (P<0.001; N = 30 for each condition). Bristol N2 worms are depicted in black, *hsf-1(sy441)* in grey. Hatching indicates transgenic expression (transgene and promoter indicated below graph).

Figure 3. HSP-16.48 acts downstream of HSF-1 in IL2 neurons. **(A)** RNAi knockdown of the small heat shock protein (HSP), *hsp-16.48*, statistically phenocopied the ethanol sensitivity of *hsf-1* RNAi knockdown in comparison to control. RNAi was performed by feeding where controls were fed empty vector. n.s. = not significant. **(B)** Either pan-neuronal (P_{rab-3}) or IL2-specific (P_{klp-6}) expression of *hsp-16.48* rescued the *hsf-1(sy441)* mutant phenotype. Expression of an *hsp-16.48* truncation mutant (+Δ38-44) was unable to rescue. **(C)** Overexpression of *hsp-16.48* in Bristol N2 worms enhanced the ethanol stimulation of locomotion to a significantly greater extent, whereas the *hsp-16.48* truncation mutant (+Δ38-44) blocked the ethanol enhancement of locomotion. For (A)-(C), data are expressed normalised to untreated controls. For each experiment, exposure to ethanol enhanced the locomotion rate of RNAi control or Bristol N2 worms (Mann-Whitney U-test; P<0.05). * indicates significant difference in comparison to treated RNAi control or Bristol N2. Comparisons were made by one-way analysis of variance with Tukey post-hoc comparisons

(P<0.001; N = 10 (A), 30 (B) and 20 (C) for each condition). Bristol N2 worms are depicted in black, *hsf-1(sy441)* in grey. Hatching indicates transgenic expression (transgene and promoter indicated below graph).

Figure 4. Ethanol enhances locomotion through an IL2-neuron $G_{\alpha s}$-dependent signalling pathway. **(A)** Stimulation of locomotion by ethanol was blocked in $G_{\alpha s}$ mutants (*gsa-1(ce94)* and *gsa-1(ce81)*), but not in $G_{\alpha o}$ (*goa-1 (n363)*) or $G_{\alpha q}$ (*egl-30(js126)*) mutants. **(B)** Forskolin stimulated *C. elegans* Bristol N2 locomotion. Increasing concentrations of forskolin significantly (*) stimulated locomotion at 10 and 100 μM in comparison to untreated worms. **(C)** Ethanol and forskolin stimulate locomotion of Bristol N2 worms to an equivalent level and this stimulation can be blocked by addition of the PKA inhibitor H-89. * indicates significant increase from untreated. n.s = not significant. **(D)** Forskolin-dependent stimulation also requires IL2 neuron expression of *hsf-1*. The forskolin effect was absent in *hsf-1(sy441)* mutants but could be rescued by re-expression of wild-type *hsf-1* under its endogenous (P_{hsf-1}) or an IL2-specific (P_{klp-6}) promoter. Like ethanol, the forskolin effect was blocked in Bristol N2 worms by pan-neuronal (P_{rab-3}) or IL2 neuron-specific (P_{klp-6}) expression of the *hsf-1* inhibitor, *hsb-1*. The forskolin effect was also absent in $G_{\alpha s}$ mutants. **(E)** Forskolin-dependent stimulation also involved IL2 neuron expression of *hsp-16.48*. Pan-neuronal (P_{rab-3}) or IL2-specific (P_{klp-6}) overexpression of *hsp-16.48* rescued the absence of the forskolin phenotype in *hsf-1(sy441)* mutant worms. Expression of the *hsp-16.48* truncation mutant (+Δ38-44) was unable to rescue. **(F)** Overexpression of *hsp-16.48* in Bristol N2 worms enhanced the forskolin stimulation of locomotion, whereas the truncation mutant (+Δ38-44) acted in a dominant negative fashion. For each experiment (A)-(F), data are expressed normalised to untreated controls. Exposure to ethanol or forskolin enhanced the locomotion rate of Bristol N2 worms (Mann-Whitney U-test; P<0.05). * indicates significant difference in comparison to treated Bristol N2. Comparisons were made by one-
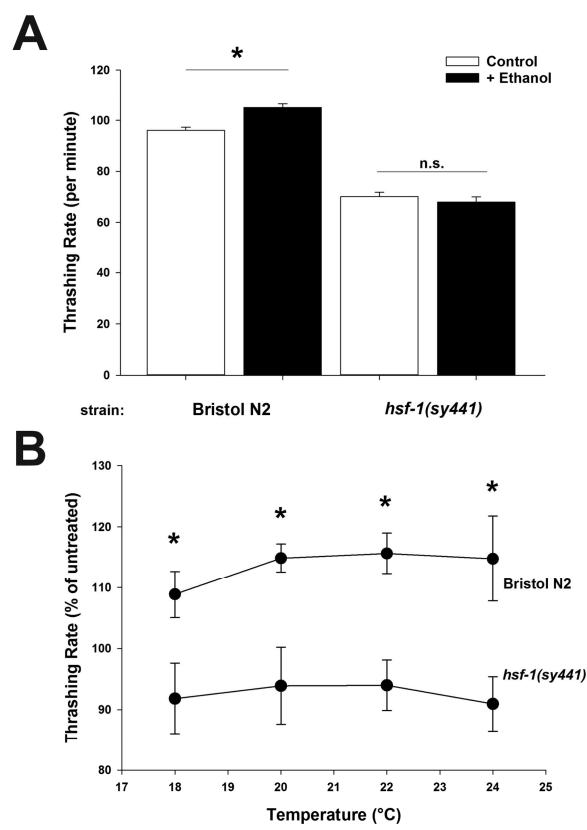
way analysis of variance with Tukey post-hoc comparisons (P<0.001; N = 20 (A, B), 25 (C, D, F) or 30 (E) for each condition). Bristol N2 worms are depicted in black, *hsf-1(sy441)* in grey. Hatching indicates transgenic expression (transgene and promoter indicated below graph).
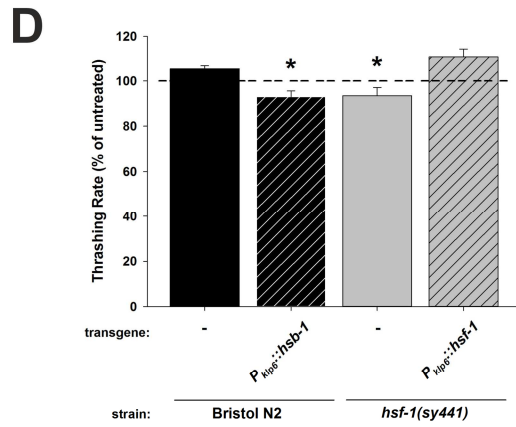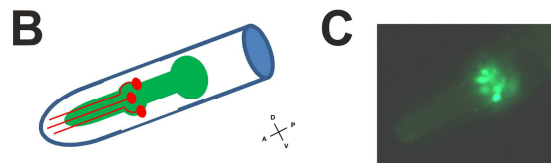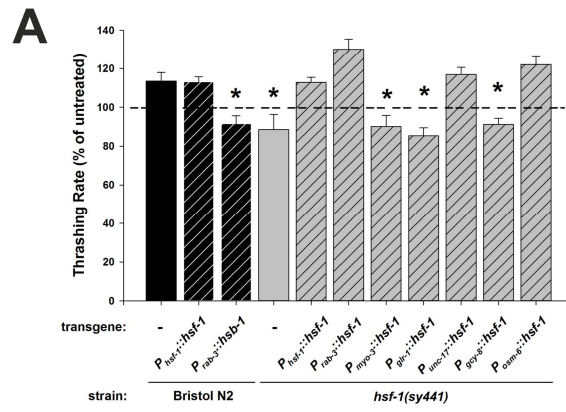
Figure 5. Ethanol enhancement of locomotion requires $G_{\alpha s}$ protein activation in IL2 neurons. ***Left.*** In control animals (*lite-1(ce314)*), addition of ethanol enhanced locomotion; however, photostimulation has no stimulatory or depressive effects. ***Middle.*** In comparison, IL2-specific optogenetic activation of $G_{\alpha s}$ stimulated *C. elegans* locomotion to an equivalent level to low ethanol exposure (*lite-1(ce314);Ex[P_{klp-6}::JellyOp]*). Simultaneous ethanol exposure and $G_{\alpha s}$ photoactivation had no additional effect on locomotion. ***Right.*** Inhibition of $G_{\alpha s}$ by IL2-specific optogenetic activation of $G_{\alpha i}$ blocked ethanol-dependent enhancement of locomotion (*lite-1(ce314);Ex[P_{klp-6}::hRh1]*). Activation of $G_{\alpha i}$ alone had no depressive effect on nematode locomotion. Addition of ethanol without $G_{\alpha i}$ activation exhibited normal locomotor enhancement. All data are expressed normalised to untreated controls. * indicates significant enhancement in comparison to untreated control. Comparisons were made by one-way analysis of variance with Tukey post-hoc comparisons (P<0.001; N = 30 for each condition). Control worms (*lite-1(ce314)*) are depicted in white, *lite-1(ce314);Ex[P_{klp-6}::JellyOp]* in black and *lite-1(ce314);Ex[P_{klp-6}::hRh1]* in grey.
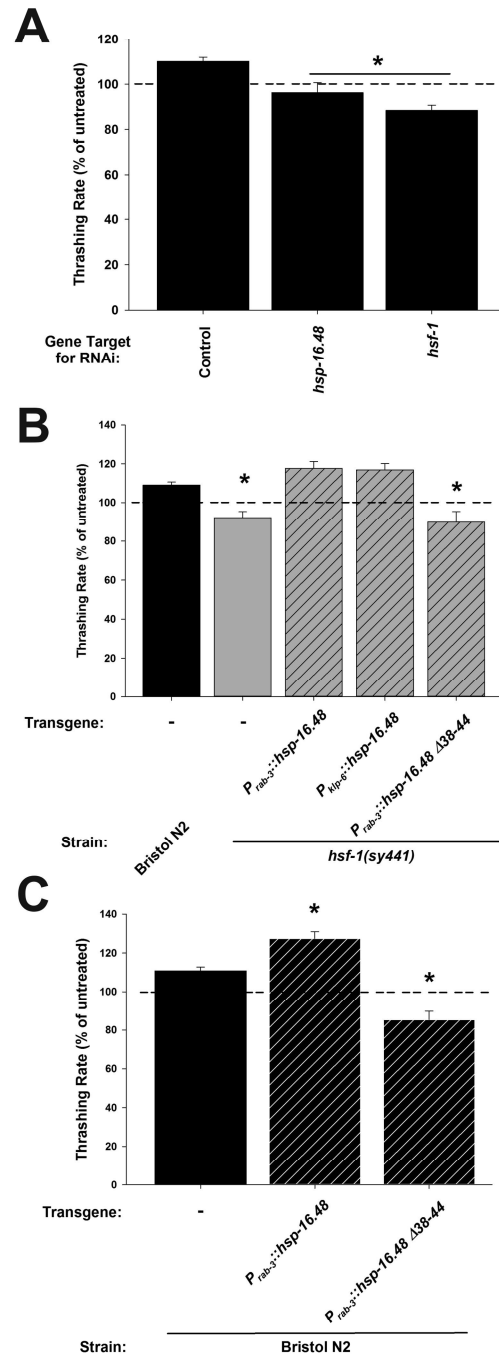
Figure 6. UNC-18 is phosphorylated by protein kinase A and phosphorylation of UNC-18 Ser322 is required for both ethanol and forskolin-dependent stimulation of locomotion. **(A)** Recombinant UNC-18 protein (GST-UNC-18) was incubated with ^{32}P-labelled ATP in the absence (mock) or presence of either protein kinase C (+PKC) or protein kinase A (+PKA). Proteins were separated by SDS-PAGE and phosphorylation was determined by PhosphorImager (Phosphoscreen). Coomassie staining indicates equal protein loading. **(B)** Liquid chromatography-MS/MS data positively indicating phosphorylation of Ser322 of
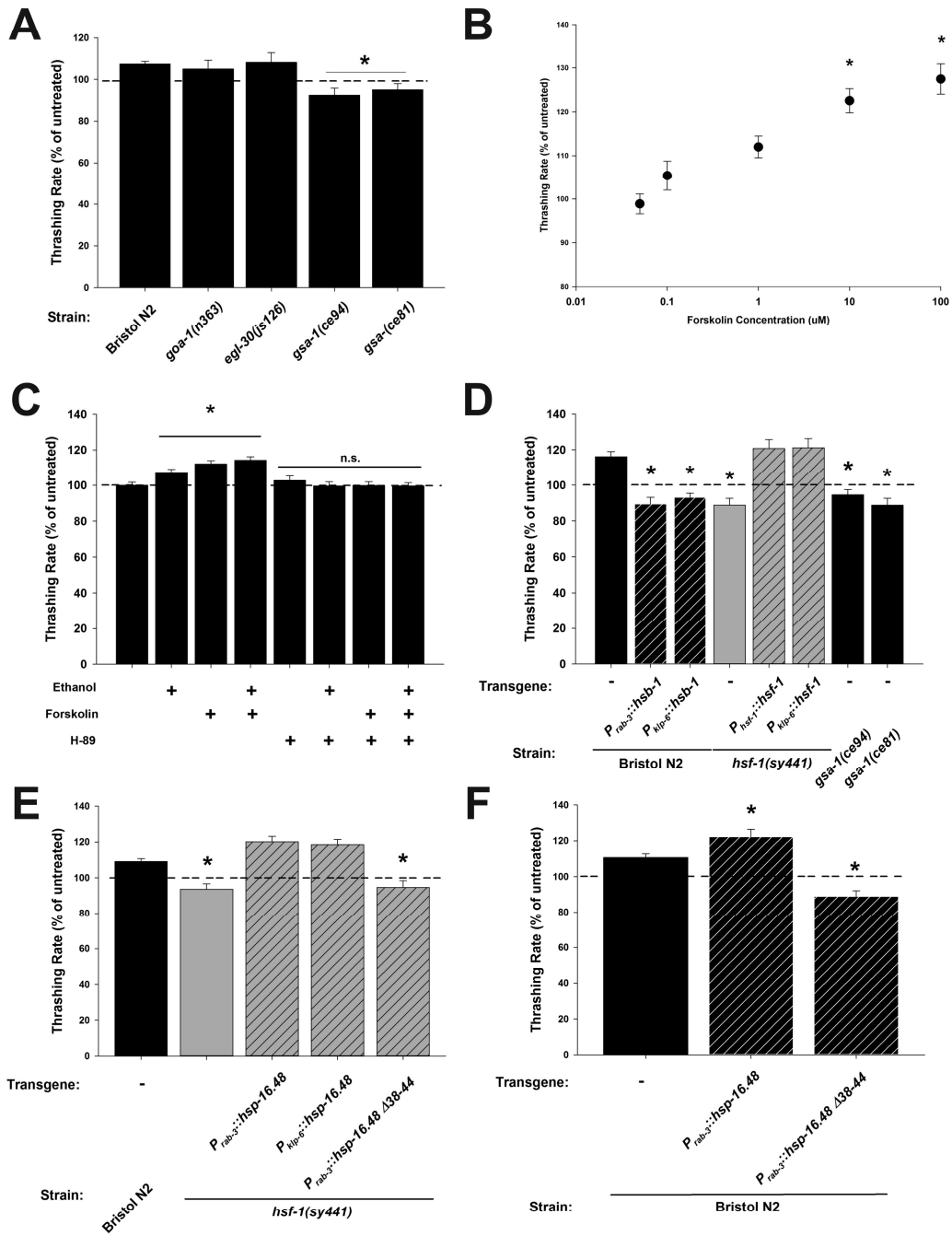
UNC-18 in PKA-phosphorylated protein samples. **(C)** Pan-neuronal ($P_{unc\text{-}18}$) or IL2-specific ($P_{klp\text{-}6}$) expression of a phospho-null mutation of a PKA-phosphorylation site of *unc-18* (S322A) in Bristol N2 blocked the ethanol-dependent stimulation of locomotion. **(D)** Pan-neuronal ($P_{unc\text{-}18}$) or IL2-specific ($P_{klp\text{-}6}$) expression of a phospho-null mutation of a PKA-phosphorylation site of *unc-18* (S322A) in Bristol N2 blocked the forskolin-dependent stimulation of locomotion. For (C) and (D), data are expressed normalised to untreated controls. Exposure to ethanol or forskolin enhanced the locomotion rate of Bristol N2 worms (Mann-Whitney U-test; $P<0.05$). * indicates significant difference in comparison to treated Bristol N2. Comparisons were made by one-way analysis of variance with Tukey post-hoc comparisons ($P<0.001$; $N = 30$ for each condition). Bristol N2 worms are depicted in black. Hatching indicates transgenic expression (transgene and promoter indicated below graph).
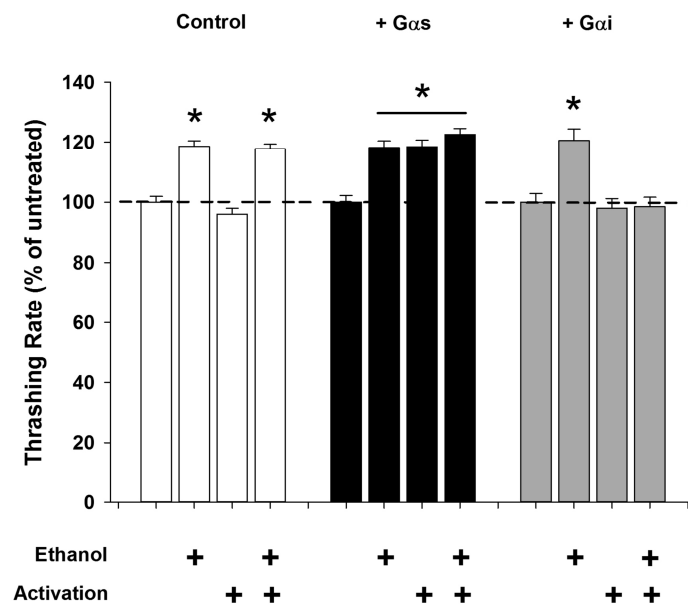
Figure 7. A model for ethanol-dependent enhancement of locomotion in *C. elegans*. The addition of ethanol at a low external concentration 17 mM activates a $G_{\alpha s}$-dependent signalling pathway in the IL2 chemosensory neurons, likely through an as yet unidentified G-protein coupled receptor. Whether ethanol directly activates or modulates an existing signal remains to be determined. The $G_{\alpha s}$-dependent signalling activates adenylyl cyclase and protein kinase A (PKA). PKA-dependent phosphorylation of the exocytotic protein UNC-18 at Ser322, in some way, alters signalling from IL2 neurons which feeds into the neurons controlling nematode locomotion.
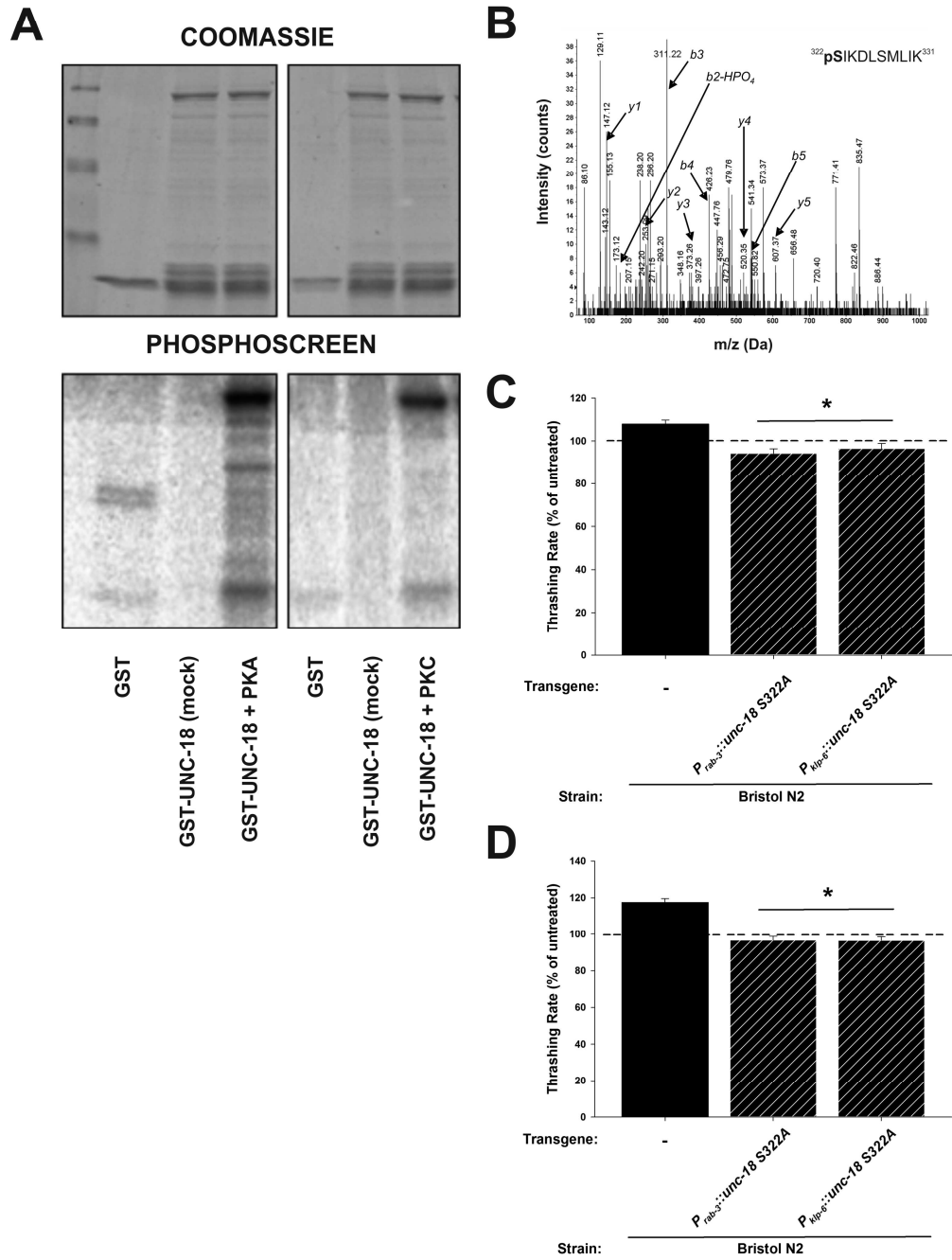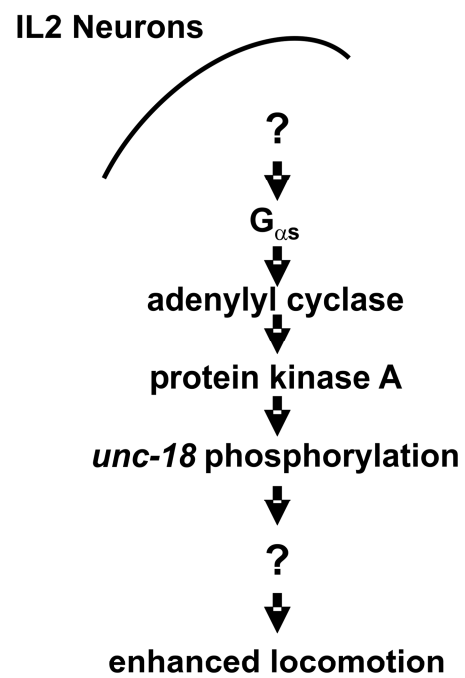
A

B

A COOMASSIE

PHOSPHOSCREEN

GST

GST-UNC-18 (mock)

GST-UNC-18 + PKA

GST

GST-UNC-18 (mock)

GST-UNC-18 + PKC

B

^{322}**pS**IKDLSMLIK^{331}

Intensity (counts)

m/z (Da)

C

Thrashing Rate (% of untreated)

Transgene: - $P_{rab-3}::unc-18\ S322A$ $P_{klp-6}::unc-18\ S322A$

Strain: Bristol N2

D

Thrashing Rate (% of untreated)

Transgene: - $P_{rab-3}::unc-18\ S322A$ $P_{klp-6}::unc-18\ S322A$

Strain: Bristol N2

IL2 Neurons

?

$G_{\alpha s}$

adenylyl cyclase

protein kinase A

***unc-18* phosphorylation**

?

enhanced locomotion

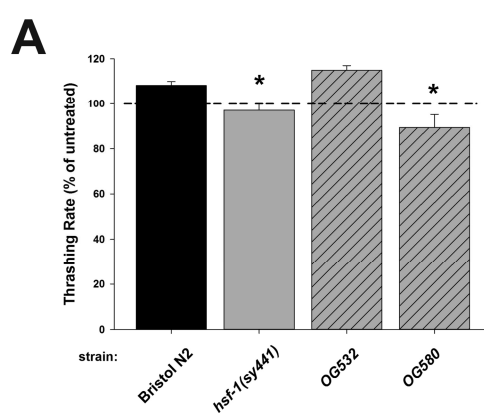**Supplemental Figure Legends**

Figure S1. Single-copy rescue of *hsf-1(sy441)* rescues the lack of ethanol and forskolin stimulation of locomotion. **(A)** The absence of ethanol stimulation in *hsf-1(sy441)* mutants was restored by single-copy expression of wild-type *hsf-1* (OG532), but not by single-copy expression of a DNA binding defective mutant of *hsf-1* (OG580). OG532 and OG580 strains were generated by Morton and Lamitina (2013). **(B)** The absence of forskolin stimulation in *hsf-1(sy441)* mutants was restored by single-copy expression of wild-type *hsf-1* (OG532), but not by single-copy expression of a DNA binding defective mutant of *hsf-1* (OG580). In both (A) and (B), data are expressed normalised to untreated controls. For each experiment, exposure to ethanol or forskolin enhanced the locomotion rate of Bristol N2 worms (Mann-Whitney U-test; $P<0.05$). * indicates significant difference in comparison to untreated Bristol N2. Comparisons were made by one-way analysis of variance with Tukey post-hoc comparisons ($P<0.001$; N = 30 for each condition). Bristol N2 worms are depicted in black, *hsf-1(sy441)* in grey. Hatching indicates single-copy rescue of *hsf-1(sy441)*.
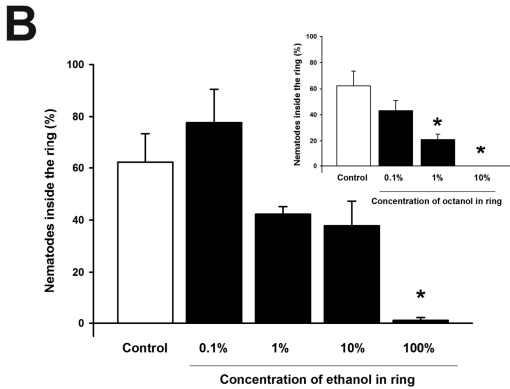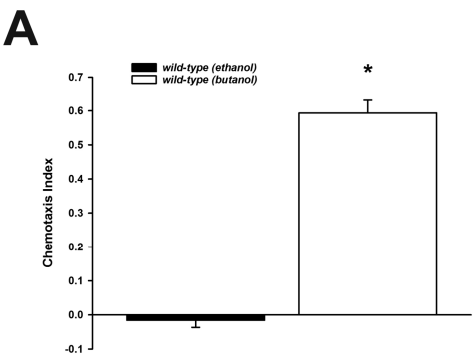
Figure S2. Ethanol does not act as a chemoattractant or chemorepellant. **(A)** In a chemotaxis assay, exposure to 100% ethanol had no effect on movement of Bristol N2 worms within 90 minutes. In comparison, 100% butanol acted as a strong chemoattractant. Comparison was made by t-test. *; $P < 0.001$ (t-test); N = 3 (butanol) and 6 (ethanol). **(B)** In an avoidance assay, Bristol N2 worms only avoided ethanol at concentrations greater than 10%. In contrast, worms avoided octanol at concentrations as low as 1% (***Inset***). * indicates significant difference in comparison to control conditions. Comparisons were made by one-way analysis of variance with Tukey post-hoc comparisons ($P<0.001$; N = 3). Control worms (exposed to distilled water) are depicted in white, alcohol exposed worms in black.
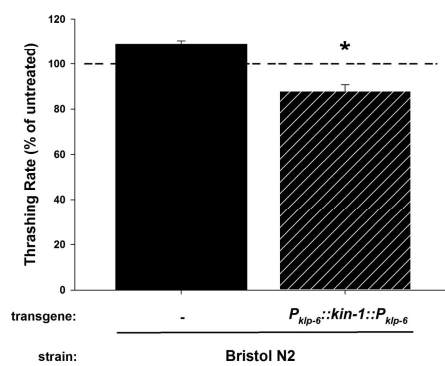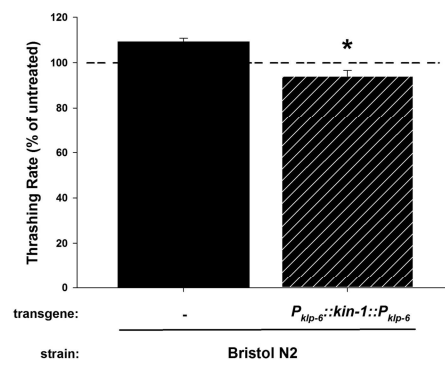
Figure S3. IL2 neuron-specific RNAi of protein kinase A (PKA) blocks ethanol and forskolin stimulation of locomotion. **(A)** IL2 neuron-specific knockdown of the catalytic subunit of *C. elegans* PKA (*kin-1*) blocked the ethanol phenotype in Bristol N2 worms. **(B)** IL2 neuron-specific knockdown of the catalytic subunit of *C. elegans* PKA (*kin-1*) blocked the forskolin phenotype in Bristol N2 worms. In both (A) and (B), data are expressed normalised to untreated controls. For each experiment, exposure to ethanol or forskolin enhanced the locomotion rate of Bristol N2 worms (Mann-Whitney U-test; $P<0.05$). * indicates significant difference in comparison to untreated Bristol N2. Comparisons were made by one-way analysis of variance with Tukey post-hoc comparisons ($P<0.001$; $N = 30$ for each condition). Bristol N2 worms are depicted in black. Hatching indicates $P_{klp-6}::kin-1::P_{klp-6}$ expression.

Table S1. Basal (untreated) thrashing rates of *C. elegans* strains used in this study. For strains grouped in parentheses, please see Table S2 for the genotypes of the individual independent transgenic lines.

Table S2. Thrashing rates of individual transgenic lines used in this study.

A

B

A

transgene: - $P_{klp\text{-}6}::kin\text{-}1::P_{klp\text{-}6}$

strain: **Bristol N2**

B

transgene: - $P_{klp\text{-}6}::kin\text{-}1::P_{klp\text{-}6}$
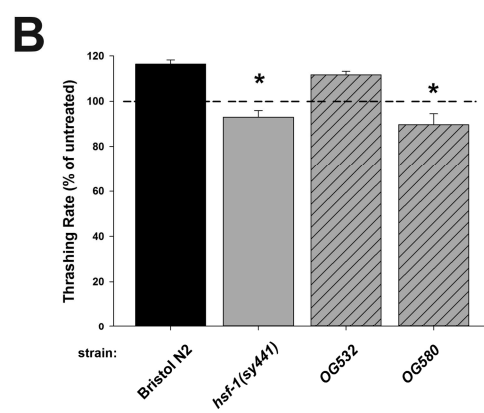
strain: **Bristol N2**

TABLES

Table S1: Basal (untreated) thrashing rates of *C. elegans* strains used in this study.

C. elegans strain	Locomotion Rate (thrashes/min)
Bristol N2	96.1±1.2
(AMG160, 161, 162) Bristol N2;*Ex[P$_{hsf-1}$::hsf-1]*	83.8±2.0
(AMG157, 158, 159) Bristol N2;*Ex[P$_{rab-3}$::hsb-1]*	83.3±2.9
(AMG475, 476, 477) Bristol N2;*Ex[P$_{klp-6}$::hsb-1]*	97.9±2.4
(AMG109, 110, 111) Bristol N2;*Ex[P$_{rab-3}$::hsp-16.48]*	75.5±4.2
(AMG142, 143, 144) Bristol N2;*Ex[P$_{rab-3}$::hsp-16.48Δ38-44]*	68.4±4.9
(AMG55, 56, 57) Bristol N2;*Ex[P$_{unc-18}$::unc-18 S322A]*	83.2±2.5
(AMG478, 479, 480) Bristol N2;*Ex[P$_{klp-6}$::unc-18 S322A]*	101.3±1.9
(AMG481, 482, 483) Bristol N2;*Ex[P$_{klp-6}$::kin-1::P$_{klp-6}$]*	89.7±2.8
PS3551 *hsf-1(sy441)*	70.1±1.6
(AMG73, 74, 75) *hsf-1(sy441);Ex[P$_{hsf-1}$::hsf-1]*	74.4±2.1
(AMG76, 77, 78) *hsf-1(sy441);Ex[P$_{rab-3}$::hsf-1]*	66.6±3.3
(AMG79, 80, 81) *hsf-1(sy441);Ex[P$_{myo-3}$::hsf-1]*	61.5±3.4
(AMG85, 86, 87) *hsf-1(sy441);Ex[P$_{glr-1}$::hsf-1]*	67.8±2.3
(AMG82, 83, 84) *hsf-1(sy441);Ex[P$_{unc-17}$::hsf-1]*	65.3±2.6
(AMG91, 92, 93) *hsf-1(sy441);Ex[P$_{gcy-8}$::hsf-1]*	61.6±2.2
(AMG88, 89, 90) *hsf-1(sy441);Ex[P$_{osm-6}$::hsf-1]*	60.9±4.1
(AMG94, 95, 96) *hsf-1(sy441);Ex[P$_{klp-6}$::hsf-1]*	80.8±4.3
(AMG97, 98, 99) *hsf-1(sy441);Ex[P$_{rab-3}$::hsp-16.48]*	64.7±2.0
(AMG469, 470, 471) *hsf-1(sy441);Ex[P$_{rab-3}$::hsp-16.48 Δ38-44]*	63.2±2.8
(AMG472, 473, 474) *hsf-1(sy441);Ex[P$_{klp-6}$::hsp-16.48]*	70.2±2.7
OG532 *hsf-1(sy441);drSi13[hsf-1p::hsf-1::GFP::unc-54 3'UTR + Cbr-unc-119(+)]*	87.7±6.8
OG580 *hsf-1(sy441);drSi28[hsf-1p::hsf-1(R145A)::GFP::unc-54 3'UTR + Cbr-unc-119(+)]*	53.6±4.1
MT363 *goa-1(n363)*	63.1±4.0
NM1380 *egl-30(js126)*	70.0±2.5
KG524 *gsa-1(ce94)*	133.3±7.9
KG421 *gsa-1(ce81)*	152.9±5.4
KG1180 *lite-1(ce314)*	47.2±0.9
AMG484 *lite-1(ce314);Ex[Pklp-6::JellyOp]*	40.7±0.9
AMG 487 *lite-1(ce314);Ex[Pklp-6::hRh1]*	38.2±1.1
NL2099 *rrf-3(pk1426) (empty vector RNAi)*	92.1±2.5
NL2099 *rrf-3(pk1426) (hsf-1 RNAi)*	93.7±1.8
NL2099 *rrf-3(pk1426) (hsp-16.48 RNAi)*	88.7±2.5

Table S2: Thrashing rates of individual transgenic lines used in this study.

C. elegans transgenic line	Locomotion Rate – untreated (thrashes per minute)	Locomotion Rate – ethanol (thrashes per minute)
AMG160 Bristol N2;*ulvEx160[P_{hsf-1}::hsf-1]*	76.0±2.4	91.2±4.7
AMG161 Bristol N2;*ulvEx161[P_{hsf-1}::hsf-1]*	87.5±3.6	95.1±3.9
AMG162 Bristol N2;*ulvEx162[P_{hsf-1}::hsf-1]*	87.9±3.5	94.3±3.6
AMG157 Bristol N2;*ulvEx157[P_{rab-3}::hsb-1]*	85.5±3.1	76.7±5.3
AMG158 Bristol N2;*ulvEx158[P_{rab-3}::hsb-1]*	73.4±5.8	64.4±7.9
AMG159 Bristol N2;*ulvEx159[P_{rab-3}::hsb-1]*	92.0±3.5	84.9±4.5
AMG475 Bristol N2;*ulvEx475[P_{klp-6}::hsb-1]*	96.4±5.4	92.0±4.0
AMG476 Bristol N2;*ulvEx476[P_{klp-6}::hsb-1]*	97.5±4.3	95.4±4.3
AMG477 Bristol N2;*ulvEx477[P_{klp-6}::hsb-1]*	99.9±2.8	85.5±4.9
AMG109 Bristol N2;*ulvEx109[P_{rab-3}::hsp-16.48]*	74.8±6.8	103.8±4.4
AMG110 Bristol N2;*ulvEx110[P_{rab-3}::hsp-16.48]*	76.6±4.8	90.9±4.0
AMG111 Bristol N2;*ulvEx111[P_{rab-3}::hsp-16.48]*	76.1±7.5	82.9±5.1
AMG142 Bristol N2;*ulvEx142[P_{rab-3}::hsp-16.48Δ38-44]*	55.8±6.3	47.6±3.8
AMG143 Bristol N2;*ulvEx143[P_{rab-3}::hsp-16.48Δ38-44]*	80.9±5.1	77.5±5.5
AMG144 Bristol N2;*ulvEx144[P_{rab-3}::hsp-16.48Δ38-44]*	71.0±3.2	63.4±10.2
AMG55 Bristol N2;*ulvEx55[P_{unc-18}::unc-18 S322A]*	84.8±4.4	79.4±3.6
AMG56 Bristol N2;*ulvEx56[P_{unc-18}::unc-18 S322A]*	76.2±3.0	72.2±3.5
AMG57 Bristol N2;*ulvEx57[P_{unc-18}::unc-18 S322A]*	88.6±4.8	83.6±2.5
AMG478 Bristol N2;*ulvEx478[P_{klp-6}::unc-18 S322A]*	104.2±3.7	101.5±4.7
AMG479 Bristol N2;*ulvEx479[P_{klp-6}::unc-18 S322A]*	96.4±2.8	93.5±5.0
AMG480 Bristol N2;*ulvEx480[P_{klp-6}::unc-18 S322A]*	103.4±2.7	98.3±3.0
AMG481 Bristol N2;*ulvEx481[P_{klp-6}::kin-1::P_{klp-6}]*	84.2±2.9	75.0±3.6
AMG482 Bristol N2;*ulvEx482[P_{klp-6}::kin-1::P_{klp-6}]*	103.3±4.8	89.8±4.7
AMG483 Bristol N2;*ulvEx483[P_{klp-6}::kin-1::P_{klp-6}]*	81.7±3.8	71.7±5.0
**AMG73 ***hsf-1(sy441);ulvEx73[P_{hsf-1}::hsf-1]*	64.6±4.3	66.4±3.5
**AMG74 ***hsf-1(sy441);ulvEx74[P_{hsf-1}::hsf-1]*	84.8±3.1	90.2±2.8
**AMG75 ***hsf-1(sy441);ulvEx75[P_{hsf-1}::hsf-1]*	66.0±3.2	82.0±2.8
**AMG76 ***hsf-1(sy441);ulvEx76[P_{rab-3}::hsf-1]*	79.8±3.6	91.4±2.1
**AMG77 ***hsf-1(sy441);ulvEx77[P_{rab-3}::hsf-1]*	80.2±3.7	90.2±3.9

AMG78 *hsf-1(sy441);ulvEx78[P$_{rab-3}$::hsf-1]*	64.8±5.1	108.4±2.4
AMG79 *hsf-1(sy441);ulvEx79[P$_{myo-3}$::hsf-1]*	58.9±6.1	55.6±8.6
AMG80 *hsf-1(sy441);ulvEx80[P$_{myo-3}$::hsf-1]*	66.2±8.3	58.2±6.0
AMG81 *hsf-1(sy441);ulvEx81[P$_{myo-3}$::hsf-1]*	59.4±2.4	52.6±2.3
AMG85 *hsf-1(sy441);ulvEx85[P$_{glr-1}$::hsf-1]*	71.3±6.3	66.9±5.1
AMG86 *hsf-1(sy441);ulvEx86[P$_{glr-1}$::hsf-1]*	67.4±2.2	60.0±2.1
AMG87 *hsf-1(sy441);ulvEx87[P$_{glr-1}$::hsf-1]*	64.6±2.2	58.6±2.5
AMG82 *hsf-1(sy441);ulvEx82[P$_{unc-17}$::hsf-1]*	69.3±5.9	94.1±5.4
AMG83 *hsf-1(sy441);ulvEx83[P$_{unc-17}$::hsf-1]*	62.4±4.6	75.6±1.9
AMG84 *hsf-1(sy441);ulvEx84[P$_{unc-17}$::hsf-1]*	64.2±2.5	69.4±1.7
AMG91 *hsf-1(sy441);ulvEx91[P$_{gcy-8}$::hsf-1]*	65.8±5.6	58.8±6.8
AMG92 *hsf-1(sy441);ulvEx92[P$_{gcy-8}$::hsf-1]*	58.0±2.1	49.8±1.8
AMG93 *hsf-1(sy441);ulvEx93[P$_{gcy-8}$::hsf-1]*	61.0±2.7	50.2±2.0
AMG88 *hsf-1(sy441);ulvEx88[P$_{osm-6}$::hsf-1]*	62.5±7.8	69.9±4.3
AMG89 *hsf-1(sy441);ulvEx89[P$_{osm-6}$::hsf-1]*	63.1±8.0	75.6±4.4
AMG90 *hsf-1(sy441);ulvEx90[P$_{osm-6}$::hsf-1]*	57.0±5.9	68.0±3.0
AMG94 *hsf-1(sy441);ulvEx94[P$_{klp-6}$::hsf-1]*	79.7±4.0	92.5±4.1
AMG95 *hsf-1(sy441);ulvEx95[P$_{klp-6}$::hsf-1]*	80.9±4.3	89.4±3.1
AMG96 *hsf-1(sy441);ulvEx96[P$_{klp-6}$::hsf-1]*	80.8±5.7	96.4±5.3
AMG97 *hsf-1(sy441);ulvEx97[P$_{rab-3}$::hsp-16.48]*	63.5±3.9	73.1±4.5
AMG98 *hsf-1(sy441);ulvEx98[P$_{rab-3}$::hsp-16.48]*	65.2±2.9	78.5±4.1
AMG99 *hsf-1(sy441);ulvEx99[P$_{rab-3}$::hsp-16.48]*	65.6±3.6	77.1±3.3
AMG469 *hsf-1(sy441);ulvEx469[P$_{rab-3}$::hsp-16.48 Δ38-44]*	58.6±3.7	50.9±6.3
AMG470 *hsf-1(sy441);ulvEx470[P$_{rab-3}$::hsp-16.48 Δ38-44]*	62.0±4.7	60.5±6.9
AMG471 *hsf-1(sy441);ulvEx471[P$_{rab-3}$::hsp-16.48 Δ38-44]*	68.9±5.7	58.5±4.9
AMG472 *hsf-1(sy441);ulvEx472[P$_{klp-6}$::hsp-16.48]*	67.2±4.5	73.5±3.5
AMG473 *hsf-1(sy441);ulvEx473[P$_{klp-6}$::hsp-16.48]*	76.4±5.2	88.2±3.5
AMG474 *hsf-1(sy441);ulvEx474[P$_{klp-6}$::hsp-16.48]*	66.9±4.3	84.2±4.3